QUANTITATIVE FINANCE
RESEARCH CENTRE

UNIVERSITY OF
TECHNOLOGY SYDNEY

QUANTITATIVE FINANCE RESEARCH CENTRE

Research Paper 390 January 2018

Time-Varying Economic Dominance Through Bistable Dynamics

Xue-Zhong He, Kai Li and Chuncheng Wang

ISSN 1441-8010 www.qfrc.uts.edu.au

TIME-VARYING ECONOMIC DOMINANCE THROUGH BISTABLE DYNAMICS

XUE-ZHONG HE*, KAI LI* AND CHUNCHENG WANG**

*University of Technology Sydney
Business School, Finance Discipline Group
PO Box 123, Broadway, NSW 2007, Australia
**Harbin Institute of Technology
Department of Mathematics
Harbin 150001, Heilongjiang, China
tony.he1@uts.edu.au
kai.li@uts.edu.au
wangchuncheng@hit.edu.cn

ABSTRACT. By developing a continuous-time heterogeneous agent model of multi-assets traded by fundamental and momentum investors, we provide a potential mechanism in generating time-varying dominance between fundamental and non-fundamental in financial market. The deterministic skeleton of the nonlinear model tends to have bistable dynamics, characterized by a Bautin bifurcation, in which a locally stable fundamental steady state coexists with a locally stable limit cycle around the fundamental, leading to two very different market states. Market prices switch stochastically between the two persistent market states, leading to the coexistence of seemingly controversial efficient market and price momentum over different time periods. The model also generates other financial market stylized facts, such as spillover effects in both momentum and volatility, market booms, crashes, and correlation reduction due to cross-sectional momentum trading. Empirical evidence based on US market supports the main findings.

Date: December 31, 2017.

Acknowledgement: Financial support from the Australian Research Council (ARC) under Discovery Grant (DP130103210), the National Natural Science Foundation of China (NSFC) Grants (Nos. 11201097, 11371112, 11461024, and 71320107003) and PIRS of HIT is gratefully acknowledged. The usual caveats apply.

1. Introduction

The coexistence of puzzling and even controversial financial market anomalies and hypotheses is well documented and perfectly reflected by 2013 Nobel Laureates Eugene Fama and Robert Shiller on their controversial views on efficient market hypothesis (Fama (1970, 2014) and Shiller (2003, 2014)). In this paper, we develop a continuous-time financial market model with heterogeneous agents who trade multi-assets based on either economic fundamentals or price momentums to characterize such coexistence in financial markets. From a globally nonlinear dynamics point of view, we show that it is the coexistence of two different and locally stable market states that underlies time-varying dominance between fundamental and non-fundamental in financial markets.

Reversal and cross-section momentum are well documented in financial markets. By incorporating investment constraints, we model asset prices as nonlinear interaction of agents who trade on fundamentals and agents who trade on price momentum (either in time series or cross-section). The resulting asset price model tends to have bistable dynamics, characterized by a Bautin bifurcation, in which a locally stable fundamental steady state coexists with a locally stable limit cycle around the fundamental. Depending on market price levels and shocks, market prices display two very different market states. One characterizes small deviations of market price from the random walk fundamental price, leading market prices to be more efficient; while the other characterizes cyclical oscillations around the fundamental, enhancing cross-sectional price momentum and leading to less efficient markets. Triggered by random shocks, market prices then switch stochastically between the two persistent market states (due to their local stability), leading to the coexistence of seemingly controversial efficient market and price momentum over different time periods.

To explore the underlying mechanism on the coexistence, we conduct a detailed analysis of the global dynamics for a nonlinear financial market model and provide better understanding of the complexity of market behavior. The analysis complements local stability analysis well documented in extant nonlinear economic model literature. By applying normal form method and center manifold theory, we demonstrate bistable dynamics (the coexistence of a locally stable steady state and a locally stable limit cycle) through a Bautin bifurcation (generalized Hopf bifurcation).[1] We provide analytical conditions for the bistable dynamics and show that both time series and cross-sectional momentum can lead to bistable dynamics. The Bautin bifurcation is characterized numerically by conditions in which a Hopf bifurcation occurs and meanwhile the first Lyapunov coefficient is zero. With the aid of the

[1]The Bautin bifurcation is similar to the Chenciner bifurcation in discrete-time model, which is used to explain the volatility clustering observed in various financial markets, see Gaunersdorfer, Hommes and Wagener (2008) and He, Li and Wang (2016).

Matlab package DDE-BIFTOOL, we numerically study the global extension of bifurcated periodic solutions, track unstable limit cycles, and provide the condition for bistable dynamics.

The current agent based financial market literature is mainly based on local stability analysis by focusing on the forward and stable bifurcated cycles. However, when the first Lyapunov coefficient is positive, the Hopf bifurcation is backward and the bifurcated periodic solution becomes unstable. In this case, the bifurcated unstable periodic solution can be extended backward with respect to bifurcation parameter until a threshold value and then the extended periodic solution becomes forward (with respect to the bifurcation parameter) and stable. Therefore, the stable fundamental steady state can coexist with the stable forward extended periodic solution, in between the backward extended periodic solution is unstable. Correspondingly, there exists an interval for the bifurcation parameter in which the two locally stable attractors coexist. This implies that, even when the fundamental steady state is locally stable, prices need not converge to the fundamental value, but may settle down to a stable limit cycle, depending on the initial price levels. The stylized analysis method for the global dynamics used in this paper can be easily applied to other nonlinear economic models as well.

The impact of cross-section momentum trading on the bistable dynamics is investigated through three scenarios. (i) In the first scenario, two separate risky asset prices have forward and stable bifurcations before introducing cross-section momentum trading among two risky assets. When agents are allowed to trade two risky assets at the same time via the cross-sectional momentum trading, the two assets are integrated into one market. We show that the new integrated market can only have forward and stable bifurcations. (ii) In the second scenario when the two prices have backward and unstable bifurcations before integration, the integrated market can either have backward (unstable) bifurcation or forward (stable) bifurcation. (iii) In the third scenario when one risky price has backward (unstable) bifurcation and the other has forward (stable) bifurcation, the integrated market can either have backward (unstable) bifurcation or forward (stable) bifurcation. The analysis on the above scenarios shows that in addition to reducing the local stability of the steady states (meaning a smaller local stability parameter region or basin of the attraction), the momentum trading can enhance the local stability of the limit cycles (meaning a larger parameter region or basin of the attraction for the bifurcated period solution), another channel through which momentum investors destabilize the market. More specifically, we show that the cross-sectional momentum trading tends to destabilize the local stability of the fundamental steady state by reducing the the parameter region of the local stability and enhance cyclical price oscillation around the fundamental steady state.

Intuitively, the bistable dynamics is caused by the constraints faced by both fundamental and momentum investors. On the one hand, various constraints faced by the fundamental traders, such as the wealth and short-sale constraints, limit the activity of the fundamental traders and reduce the size of the basin of the local attractor of the stable fundamental steady state. When the initial values are far away from the steady state, the prices tend to depart further from the steady state. On the other hand, the wealth and short-sale constraints also limit the destabilizing role of the momentum investors. As a result, the prices cannot explode but settle down at a stable cycle when the initial prices are far away from the steady state fundamental prices. Therefore, the constraints limit the strengths of both local attractors (the stable steady state and the stable limit cycle), resulting in the bistable dynamics.

Our results lead to several empirical implications. First, we find that a strong integration via the cross-sectional momentum results in comovements in asset prices in opposite directions. Second, cross-sectional momentum trading can give rise to a spillover effect in momentum, which is documented empirically in Gebhardt, Hvidkjaer and Swaminathan (2005) and Jostova, Nikolova, Philipov and Stahel (2013), and can reduce the correlation of stock returns. More interestingly, the model suggests that cross-sectional momentum trading tends to be self-fulfilling in the sense that it destabilizes the market and generates additional price trends in cross-section. Further more, we provide empirical evidence based on US market to support the reduction in return correlation. We find that an increase in the usage of cross-sectional momentum strategies significantly decreases the correlations among stocks, an average decrease by 35% after Jegadeesh and Titman published their seminal work in 1993. Also the profits of the cross-sectional momentum increases by 1.5%. The empirical results are consistent with our analytical findings.

This paper is closely related to the momentum literature. Momentum profitability is found to depend on market states (Chordia and Shivakumar, 2002, and Cooper, Gutierrez and Hameed, 2004), investor sentiment (Antoniou, Doukas and Subrahmanyam, 2013) and market volatility (Wang and Xu, 2015). For example, Cooper, Gutierrez and Hameed (2004) find that short-run (six months) momentum strategies are profitable in an up-market, but no in a down-market. Recently, Daniel and Moskowitz (2016) document that momentum strategy tends to experience severe crashes during market rebounds. Chu, He, Li and Tu (2015) show that the dominance of fundamental and behavioral-bias-related non-fundamental strengths is time-varying.[2] However, most existing theories are independent of market conditions either implying a long-lasting momentum or ruling out the existence of momentum.

[2]He, Li and Li (2017) shows that studying both fundamental and momentum jointly is more powerful than examining each in isolation.

They are difficult to harmonize with the time-varying existence of momentum. In our model, the "inefficient" momentum and "efficient" market price can coexist, and their dominance depends on the price levels (and price shocks).

The paper is also related to heterogeneous agent models (HAMs) literature. Over the last three decades, empirical evidence, unconvincing justification of the assumption of unbounded rationality, and investor psychology have led to the growing research on HAMs.[3] With different groups of investors having different expectations about future prices, HAMs have shown that asset price fluctuations can be caused by an endogenous mechanism of interaction of heterogeneous agents (Chiarella, Dieci and Gardini (2002), and Brock and Hommes (1997, 1998)). Given the complexity of nonlinear financial markets, most of HAMs is computationally oriented based on local stability and bifurcation analysis while the globally nonlinear properties are seldom analyzed (through the normal form method and the center manifold theory).[4] This paper conducts an analysis of global dynamics, which complements the local stability analysis well documented in HAMs literature. It provides better understanding of the complexity and the underlying economic mechanism of market behavior.

The bistable dynamics is related to multiple equilibria mechanism in the sense that a nonlinear financial market can have multiple locally stable attractors. However, different from the multiple equilibria mechanism, the two attractors in our mechanism are very different. Therefore the model is able to characterize seemingly unrelated or even opposite market phenomena, such as price momentum and efficient market.

The paper is organized as follows. We first propose a continuous-time heterogeneous agent model of two assets in Section 2 to explicitly characterize momentum trading. In Section 3, we apply stability and bifurcation theory, together with normal form method and center manifold theory, to examine both local and global dynamics of the model. In particular, we demonstrate the coexistence of a local stable fundamental price and a locally stable closed cycle around the fundamental price. Section 4 conducts a numerical analysis of the stochastic model to explore the joint impact of the global deterministic dynamics and noises. Based on US market data, Section 5 provides empirical evidence to support some implications of the

[3]See Hommes (2006), LeBaron (2006), Chiarella, Dieci and He (2009), Lux (2009) and He (2013) for surveys of the recent development in this literature.

[4]He, Li, Wei and Zheng (2009) and He et al. (2016) are two exceptions. In addition to the local stability analysis, He et al. (2009) analytically examine the bifurcation properties, including the direction of the bifurcation, the stability of the bifurcated cycle, and the global extension of the bifurcated cycle. He et al. (2016) analytically provide the conditions of Chenciner bifurcation and show the coexistence of two local attractors.

model. Section 6 concludes. A more general model with multiple assets and all the proofs are included in the appendices.

2. The Model

We consider a financial market of two risky assets (A and B), populated by fundamental investors, extrapolators, and noise traders. To have an intuitive and parsimonious model, we motivate the demand functions based on agents' behavior directly by following Chiarella (1992), He and Li (2012, 2015) and Di Guilmi, He and Li (2014).[5] The fundamental investors trade based on the (log) book-to-market ratio and their excess demands are given by

$$D^i_{f,t} = \tanh[\beta_f(F^i_t - P^i_t)], \quad i = A, B, \tag{2.1}$$

where F^i_t and P^i_t are the log fundamental price and log market price respectively at time t, and $\beta_f > 0$ is a constant measuring the mean-reverting of the market price to the fundamental price. The S-shaped demand function $\tanh(\cdot)$ reflects various constraints faced by agents, such as the wealth constraint (the upper bound) and the short-sale constraint (the lower bound). For simplicity, we consider that the fundamental prices are governed by

$$\begin{pmatrix} dF^A_t \\ dF^B_t \end{pmatrix} = \Sigma^F dW^F_t, \quad \Sigma^F = \begin{pmatrix} \sigma^F_{A,1} & \sigma^F_{A,2} \\ \sigma^F_{B,1} & \sigma^F_{B,2} \end{pmatrix}, \quad \begin{pmatrix} F^A_0 \\ F^B_0 \end{pmatrix} = \begin{pmatrix} \bar{F}^A \\ \bar{F}^B \end{pmatrix}, \tag{2.2}$$

where Σ^F is the variance-covariance matrix for fundamental returns and $W^F_t = (W^F_{1,t}, W^F_{2,t})'$ are two independent Brownian motions.

The literature has extensively documented that many individual and institutional investors extrapolate historical returns,[6] and shown that both time series momentum (or absolute momentum) and cross-sectional momentum (or relative momentum) widely used in practice can generate persistent and sizeable profits.[7] Accordingly, we also consider extrapolators in the economy who trade on short-run price trends. The extrapolators estimate price trend using a moving average of historical returns

$$\int_{t-\tau}^{t} dP^i_u = P^i_t - P^i_{t-\tau},$$

where dP^i_u is the (log) instantaneous return of asset i, and τ is the look-back period of the extrapolation. There are two types of extrapolators, based on time series

[5]The demands in the continuous-time setup are consistent with those deriving from heterogeneous expectations and utility maximization in discrete time heterogeneous agent models literature, see, for example, Brock and Hommes (1997, 1998).

[6]See, e.g., Vissing-Jorgensen (2004), Bacchetta, Mertens and van Wincoop (2009), Barberis (2013), Amromin and Sharpe (2014), Greenwood and Shleifer (2014) and Kuchler and Zafar (2016).

[7]See, e.g., Jegadeesh and Titman (1993) and Moskowitz, Ooi and Pedersen (2012) among many others.

momentum (or absolute momentum) and cross-sectional momentum (or relative momentum) respectively. The demands of the absolute momentum investors for asset A and B are given, respectively, by

$$D_{a,t}^i = \tanh[\beta_a(P_t^i - P_{t-\tau}^i)], \quad i = A, B, \tag{2.3}$$

where parameter $\beta_a > 0$ represents the extrapolation rate of the absolute momentum investors on the future price trend. The demands of the cross-sectional momentum investors are given by

$$\begin{aligned} D_{c,t}^A &= \tanh\{\beta_c[(P_t^A - P_{t-\tau}^A) - (P_t^B - P_{t-\tau}^B)]\}, \\ D_{c,t}^B &= \tanh\{\beta_c[(P_t^B - P_{t-\tau}^B) - (P_t^A - P_{t-\tau}^A)]\}, \end{aligned} \tag{2.4}$$

where $\beta_c > 0$ is a constant. Equation (2.4) implies that the cross-sectional momentum strategy is a zero-investment strategy by taking a long position in one asset and short position in the other asset simultaneously. We consider the same time horizon τ for both assets to be consistent with the cross-sectional momentum literature.

Therefore, both fundamental investors and absolute momentum investors focus on only individual asset, while the cross-sectional momentum investors trade on two assets simultaneously. The market fractions of the three types of investors who trade on asset i are α_f^i, α_a^i and α_c^i respectively, satisfying $\alpha_f^i + \alpha_a^i + \alpha_c^i = 1$. Notice α_c^i measures the market fraction rather than the number of traders. So it can be different for the two assets even though the cross-sectional momentum investors are the same group of investors across the two risky assets.

The market maker adjusts the market price according to the aggregated excess demand

$$\begin{aligned} dP_t^A = \mu^A \Big[& \alpha_f^A \tanh[\beta_f(F_t^A - P_t^A)] + \alpha_a^A \tanh[\beta_a(P_t^A - P_{t-\tau}^A)] \\ & + \alpha_c^A \tanh\{\beta_c[(P_t^A - P_{t-\tau}^A) - (P_t^B - P_{t-\tau}^B)]\} \Big] dt + \sigma_A^M dW_t^M, \\ dP_t^B = \mu^B \Big[& \alpha_f^B \tanh[\beta_f(F_t^B - P_t^B)] + \alpha_a^B \tanh[\beta_a(P_t^B - P_{t-\tau}^B)] \\ & + \alpha_c^B \tanh\{\beta_c[(P_t^B - P_{t-\tau}^B) - (P_t^A - P_{t-\tau}^A)]\} \Big] dt + \sigma_B^M dW_t^M, \end{aligned} \tag{2.5}$$

where the constant $\mu^i > 0$ represents the speed of the price adjustment by the market maker, $\Sigma^M = (\sigma_A^M, \sigma_B^M)'$ is the variance-covariance matrix for the market returns and $W_t^M = (W_{1,t}^M, W_{2,t}^M)'$ represent two independent Brownian motions, measuring the demands of noise traders or market noises. They can be correlated with the fundamental shocks $W_{F,t}$. Especially, if Σ^M is a diagonal matrix, then the conditional volatility of one asset cannot be affected by the other asset and hence any spill-over effect in realized volatility cannot be introduced by this term. However, the two assets are still linked via the fundamental correlation and the relative momentum investors.

The asset price model (2.5) is characterized by a nonlinear stochastic delay differential system. The resulting returns are linear functions of three factors, including a fundamental component and two momentum components, in addition to a noise term.[8] In the following analysis, the local dynamics of the corresponding deterministic model are examined via the linearized form of (2.5). We show that, different from the fundamental factor, the two momentum factors tend to destabilize the market and may result in non-stationary return processes. Furthermore, the global dynamics analysis shows a rich and more complex return behavior, which can be beyond the scope of the linear models used in the empirical momentum literature.

3. Deterministic Dynamics

This section examines the price dynamics of the deterministic skeleton of (2.5). By assuming a constant fundamental price $F_t^i = \bar{F}^i$ and no market noise $\Sigma^M = 0$, system (2.5) becomes a deterministic system of delay differential equations, representing the mean processes of market returns of the two risky assets

$$\begin{aligned}
\dot{P}_t^A &= \mu^A \Big[\alpha_f^A \tanh[\beta_f(\bar{F}^A - P_t^A)] + \alpha_a^A \tanh[\beta_a(P_t^A - P_{t-\tau}^A)] \\
&\qquad + \alpha_c^A \tanh\{\beta_c[(P_t^A - P_{t-\tau}^A) - (P_t^B - P_{t-\tau}^B)]\}\Big], \\
\dot{P}_t^B &= \mu^B \Big[\alpha_f^B \tanh[\beta_f(\bar{F}^B - P_t^B)] + \alpha_a^B \tanh[\beta_a(P_t^B - P_{t-\tau}^B)] \\
&\qquad + \alpha_c^B \tanh\{\beta_c[(P_t^B - P_{t-\tau}^B) - (P_t^A - P_{t-\tau}^A)]\}\Big].
\end{aligned} \tag{3.1}$$

The linearization of (3.1) at its unique fundamental steady state $(P^A, P^B) = (\bar{F}^A, \bar{F}^B)$ is given by

$$\begin{aligned}
\dot{P}_t^A &= (\gamma_a^A + \gamma_c^A - \gamma_f^A)P_t^A - (\gamma_a^A + \gamma_c^A)P_{t-\tau}^A - \gamma_c^A P_t^B + \gamma_c^A P_{t-\tau}^B, \\
\dot{P}_t^B &= (\gamma_a^B + \gamma_c^B - \gamma_f^B)P_t^B - (\gamma_a^B + \gamma_c^B)P_{t-\tau}^B - \gamma_c^B P_t^A + \gamma_c^B P_{t-\tau}^A,
\end{aligned} \tag{3.2}$$

where $\gamma_f^i = \mu^i \alpha_f^i \beta_f$, $\gamma_a^i = \mu^i \alpha_a^i \beta_a$ and $\gamma_c^i = \mu^i \alpha_c^i \beta_c$, $i = A, B$, measure the activities of the three types of investors. Before studying the full model (3.1) with all three types of investors, we first examine several special cases to understand the roles of different types of traders.

[8] In a different setup of consumption-based capital asset pricing model where sentiment investors extrapolate the expected returns using all historical returns, Barberis, Greenwood, Jin and Shleifer (2015) show that the return process is linear in the dividend process and the extrapolators' belief. Empirically, Grinblatt and Moskowitz (2004) and Heston and Sadka (2008), among others, find that the historical average returns over a short-run horizon can positively forecast the cross-section of expected returns.

3.1. **Bistable Dynamics of the Single Asset Model.** We first consider the case when there is no relative momentum investors, that is $\gamma_c^i = 0$. In this case, the price dynamics of the two assets are decoupled into two separate single asset price dynamics,

$$\begin{aligned} \dot{P}_t^A &= \mu^A\Big[\alpha_f^A \tanh[\beta_f(\bar{F}^A - P_t^A)] + \alpha_a^A \tanh[\beta_a(P_t^A - P_{t-\tau}^A)]\Big], \\ \dot{P}_t^B &= \mu^B\Big[\alpha_f^B \tanh[\beta_f(\bar{F}^B - P_t^B)] + \alpha_a^B \tanh[\beta_a(P_t^B - P_{t-\tau}^B)]\Big]. \end{aligned} \tag{3.3}$$

The local dynamics can be described by the following proposition.

Proposition 3.1. *For system* (3.3) *with* $i = A, B$*,*

(1) *it has a unique fundamental steady state* $P^i = \bar{F}^i$*;*
(2) *the fundamental steady state* P^i *is locally asymptotically stable for all* $\tau \geq 0$ *when* $\gamma_f^i \geq 2\gamma_a^i$*;*
(3) *the fundamental steady state* P^i *is locally asymptotically stable for* $\tau < \tau_0^i$ *and unstable for* $\tau > \tau_0^i$ *when* $\gamma_f^i < 2\gamma_a^i$*. In addition,* P^i *undergoes Hopf bifurcations at* $\tau = \tau_n^i$*,* $n = 0, 1, 2, \cdots$*.*

Local dynamics have been well understood in the HAMs literature. For example, He and Li (2012), among others, show that fundamental investors play a stabilizing role while momentum investors play a destabilizing role in financial markets, and the local stability switches as the time horizon τ increases. Especially, if neither absolute momentum investors nor relative momentum investors participate into the market, the fundamental steady state is always stable.

However, global price dynamics have been seldom studied in the literature[9] and are still unclear so far. Therefore, we mainly focus on global dynamics, the coexistence of attractors and the interaction between the two asset dynamics in this paper. Denote the first Lyapunov coefficient by $c_1(0)$, which is derived in Appendix B.2. The properties of the Hopf bifurcation is given by the following proposition.

Proposition 3.2. *For system* (3.3) *with* $i = A, B$*,*

(1) *if* $c_1(0) = 0$*, it undergoes a Bautin bifurcation (generalized Hopf bifurcation);*
(2) *if* $\gamma_f^i < 2\gamma_a^i$ *and* $c_1(0) \neq 0$*, then the direction and stability of bifurcated periodic solutions (Hopf bifurcation) are completely determined by the sign of* $c_1(0)$*. That is, the bifurcated periodic solutions is forward stable when* $c_1(0) < 0$*, but backward and unstable when* $c_1(0) > 0$*.*

Fig. 3.1 illustrates the impact of absolute momentum trading, measured by β_a, on the global price dynamics, especially the stability of the limit cycles. As β_a increases, the sign of the first Lyapunov coefficient $c_1(0)$ switches from positive to negative.

[9]He et al. (2009) and He et al. (2016) are two exceptions.

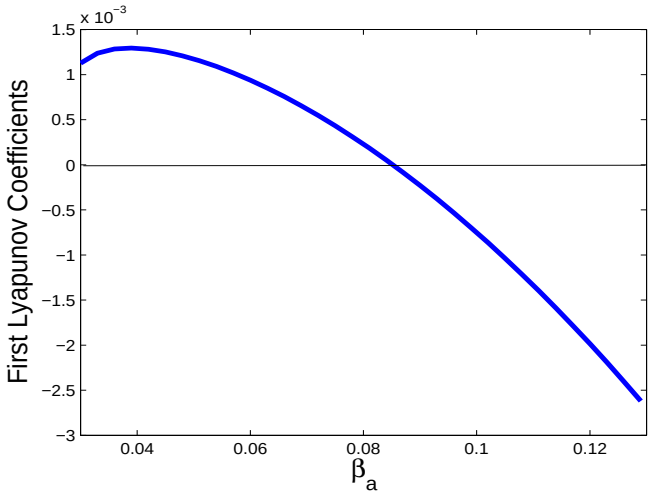

FIGURE 3.1. First Lyapunov coefficient as a function of β_a. Here $\mu^i = 15$, $\alpha_f^i = 0.2$, $\alpha_a^i = 0.8$, $\alpha_c^i = 0$, $\beta_f = 0.2$ and $\tau = \tau_0^i$.

Following Proposition 3.2, the direction of Hopf bifurcation changes from backward to forward; correspondingly the unstable bifurcated cycle becomes stable. When the first Lyapunov coefficient $c_1(0) = 0$, the system (3.3) has a Bautin bifurcation (generalized Hopf bifurcation). The occurrence of Bautin bifurcation implies that, with proper set of parameters, a stable steady state can coexists with a stable limit cycle (a bistable dynamics, see Chapter 8 of Kuznetsov (2004)). Interestingly, numerical simulations suggest that the first Lyapunov coefficient $c_1(0)$ tends to keep the same sign as α_j^i varies. Intuitively, the right-hand side of (3.3) is linear in α_j^i, implying that α_j^i can affect the local stability of the steady state while may not affect the stability of the bifurcation. However, (3.3) is nonlinear in β_j and hence can affect the global dynamics as illustrated in Fig. 3.1. In the following analysis, we examine two different scenarios ($c_1(0) > 0$ and $c_1(0) < 0$) separately, and show that these two scenarios have different local and global dynamics.

3.1.1. *Scenario 1:* $c_1(0) > 0$. We set $\mu = \mu^i = 15$, $\alpha_f^i = 0.2$, $\alpha_a^i = 0.8$, $\alpha_c^i = 0$, $\beta_f = 0.2$ and $\beta_a = 0.04$. It follows from (B.5) and (B.11) that the first Hopf bifurcation value $\tau_0 \approx 3.92$ and first Lyapunov coefficient $c_1(0) = 1.3 \times 10^{-3} > 0$. Proposition 3.1 states that the fundamental steady state is locally stable for $\tau < \tau_0^i$ and becomes unstable for $\tau > \tau_0^i$. Proposition 3.2 further shows that there is a backward Hopf bifurcation when $\tau = \tau_0^i$, and the corresponding bifurcated periodic solution is unstable. We numerically examine the tendency of the bifurcated periodic solution using the Matlab package DDE-BIFTOOL, which can even track the unstable limit cycles. The numerical method is described in Appendix B.3. Fig. 3.2 illustrates how the bifurcated periodic solution varies with parameter τ. Every point in the curve stands for a periodic solution, and hence the curve is called the

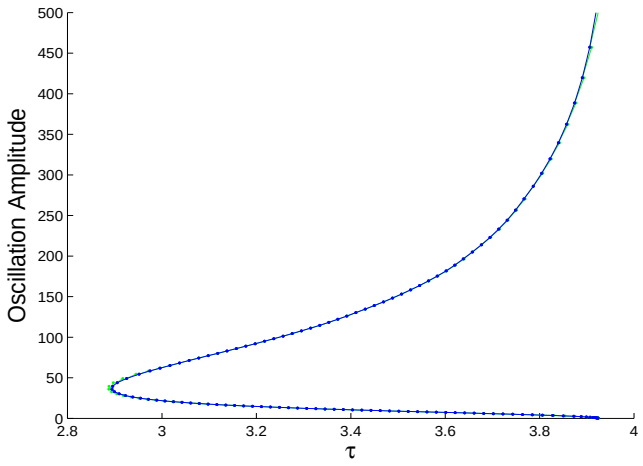

FIGURE 3.2. The extension of periodic solution bifurcated through a backward and unstable Hopf bifurcation. Here $\mu = \mu^i = 15$, $\alpha_f^i = 0.2$, $\alpha_a^i = 0.8$, $\alpha_c^i = 0$, $\beta_f = 0.2$ and $\beta_a = 0.04$. The first Hopf bifurcation value $\tau_0^i \approx 3.92$ and first Lyapunov coefficient $c_1(0) = 1.3 \times 10^{-3} > 0$.

branch of periodic solutions.[10] As τ varies, the periodic solution with small amplitude at the beginning, moves to the left initially, then turn around at the critical value $\tau^{i*}(\approx 2.89)$, and shift to the right. At $\tau = \tau^{i*}$, the two limit cycles collide and disappear via a saddle-node bifurcation of periodic solutions (Kuznetsov, 2004). Therefore, two periodic solutions coexist for $\tau \in (\tau^{i*}, \tau_0^i)$. By further computing the corresponding nontrivial Floquet multiplier (the one with the maximal module among all multipliers) for these two periodic solutions with fixed $\tau \in (\tau^{i*}, \tau_0^i)$, we find that the periodic solution with relatively larger amplitude is stable, while the other is unstable. Hence, when τ is within the 'coexistence interval' (τ^{i*}, τ_0^i), there are two local attractors, the asymptotically stable fundamental steady state and the asymptotically stable limit cycle with larger amplitude, and in between there is an unstable cycle. As τ increases, the branch increases steeply, implying large amplitudes of the cycles. Numerical simulations (not reported here) show that an increase in β_a decreases the length of the coexistence interval.

The bistable dynamics are caused by the limited activities of both fundamental and momentum investors. Intuitively, on the one hand, the fundamental investors face various constraints, such as the wealth and short-sale constraints, which limit the activity of the fundamental investors and reduce the size of the basin of the local attractor of the stable steady state. When the initial values are far away from the steady state, the prices tend to further depart from the steady state. On the other hand, the wealth and short-sale constraints (or the S-shaped demand function) also

[10]We refer readers to He et al. (2009) for the proofs of the global extension of Hopf bifurcation.

limit the destabilizing role of the momentum investors. As a result, the prices cannot explode to infinity but will settle down at a stable cycle when the initial values are far away from the steady state. Therefore, the constraints limit the strengths of both local attractors (the stable steady state and the stable limit cycle), resulting in the bistable dynamics.[11] In the following section, we will show that, triggered by the random shocks in the full stochastic model (2.5), the bistable dynamics can lead market prices to switch stochastically but persistently between the two attractors, characterizing two very different market states.

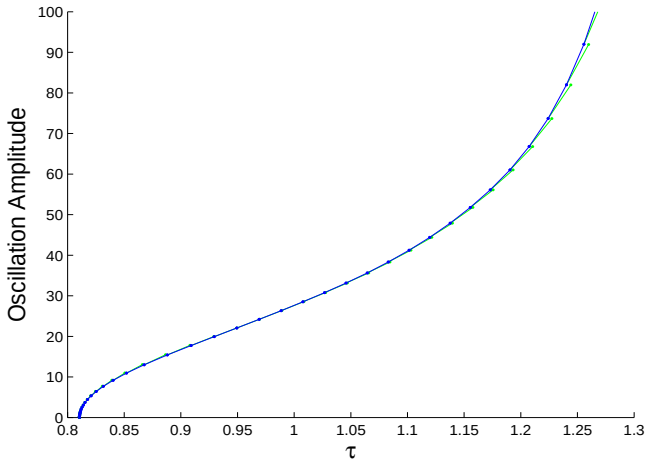

FIGURE 3.3. The extension of periodic solution bifurcated through a forward and stable Hopf bifurcation. Here $\mu = \mu^i = 15$, $\alpha_f^i = 0.2$, $\alpha_a^i = 0.8$, $\alpha_c^i = 0$, $\beta_f = 0.2$ and $\beta_a = 0.12$. The first Hopf bifurcation value $\tau_0^i \approx 0.81$ and first Lyapunov coefficient $c_1(0) = -2.0 \times 10^{-3} < 0$.

3.1.2. *Scenario 2:* $c_1(0) < 0$. We choose $\mu = \mu^i = 15$, $\alpha_f^i = 0.2$, $\alpha_a^i = 0.8$, $\alpha_c^i = 0$, $\beta_f = 0.2$ and $\beta_a = 0.12$. In this case, the first Hopf bifurcation value is $\tau_0^i \approx 0.81$, and $c_1(0) = -2.0 \times 10^{-3} < 0$, and Proposition 3.2 shows that the Hopf bifurcation is forward and stable. Fig. 3.3 illustrates the extension of the Hopf bifurcation. The fundamental steady state is stable for $\tau < \tau_0^i$ and becomes unstable for $\tau > \tau_0^i$. The bifurcated forward limit cycles are stable and the amplitude of the cycles increases as τ increases.

We complete the discussion with the following remark. When the Hopf bifurcation is forward and stable as in Scenario 2, the oscillation amplitude of the bifurcated cycles is very small around the bifurcation value and increases with τ. However,

[11] On the one hand, we find that the limit cycles tend to be unstable and the solutions to the system can explode to infinity without the S-shaped demand functions of the momentum investors. On the other hand, after removing the S-shaped demand functions of the fundamental investors, although the limit cycles are stable, the bistable dynamics tend to disappear.

when the Hopf bifurcation is backward and unstable as in Scenario 1, the extended bifurcated cycles have large oscillation amplitude around the bifurcation value. In other words, there is a big jump from the stable steady state to the stable cycle around the bifurcation value.

3.2. **Bistable Dynamics of the Two Assets Model.** The previous analysis shows the different roles played by different types of investors. We now analyze the market stability when all three strategies are employed. The market stability of the system (3.1) can be characterized by the following proposition.

Proposition 3.3. *For system* (3.1)*,*

(1) *it has a unique fundamental steady state* $(P^A, P^B) = (\bar{F}^A, \bar{F}^B)$*;*
(2) *the fundamental steady state is locally asymptotically stable for all* $\tau \geq 0$ *under condition* $\overline{\boldsymbol{C}}$ *defined in Appendix B.6;*
(3) *the fundamental steady state is locally asymptotically stable for* $\tau \in [0, \tau_0)$ *and becomes unstable for* $\tau > \tau_0$ *under condition* $\boldsymbol{C}$ *in Appendix B.6;*
(4) *it undergoes a Hopf bifurcation at* $\tau = \tau_0$ *under condition* $\boldsymbol{C}$*. In addition, if* $\frac{T}{c_1(0)} < 0$ *(*$\frac{T}{c_1(0)} > 0$*), then the bifurcation is forward (backward), and the bifurcated periodic solution is stable (unstable) when* $c_1(0) < 0$ *(*$c_1(0) > 0$*), where* T *and the first Lyapunov coefficient* $c_1(0)$ *are defined in Appendix B.6.*

Proposition 3.3 shows that the direction and the stability of bifurcated periodic solution is determined by the sign of both the transversality condition T and the first Lyapunov coefficient $c_1(0)$. When the two individual systems are coupled together, the market integration cannot alter the fundamental steady state of each asset, while tends to destabilize the market in the sense that the integrated market is prone to be more unstable. In the remaining analysis, we further investigate the impact of integration on price dynamics by examining the integration strength β_c.

Especially, if there is no absolute momentum investors, that is $\alpha_a^i = 0$, then Proposition 3.3 reduces to the following corollary.

Corollary 3.4. *Assume that* $\alpha_a^i = 0$ *for* $i = A, B$*.*

(1) *The fundamental steady state is locally asymptotically stable for all* $\tau \geq 0$ *when* $b_2 \geq 0$*, where* $b_2 = \gamma_f^A \gamma_f^B (\gamma_f^A \gamma_f^B - 2\gamma_f^A \gamma_c^B - 2\gamma_f^B \gamma_c^A)$*.*
(2) *The fundamental steady state is locally asymptotically stable for* $0 \leq \tau < \tau_0$ *and becomes unstable for* $\tau > \tau_0$ *when* $b_2 < 0$*. In addition, system* (3.1) *undergoes Hopf bifurcations at* $\tau = \tau_n$*,* $n = 1, 2, \cdots$*, where* τ_n *is given by* (B.21)*.*
(3) *If* $\frac{T}{c_1(0)} < 0$ *(*$\frac{T}{c_1(0)} > 0$*), then the bifurcation is forward (backward), and the bifurcated periodic solution is stable (unstable) when* $c_1(0) < 0$ *(*$c_1(0) > 0$*), where* T *and the first Lyapunov coefficient* $c_1(0)$ *are defined in Appendix B.6.*

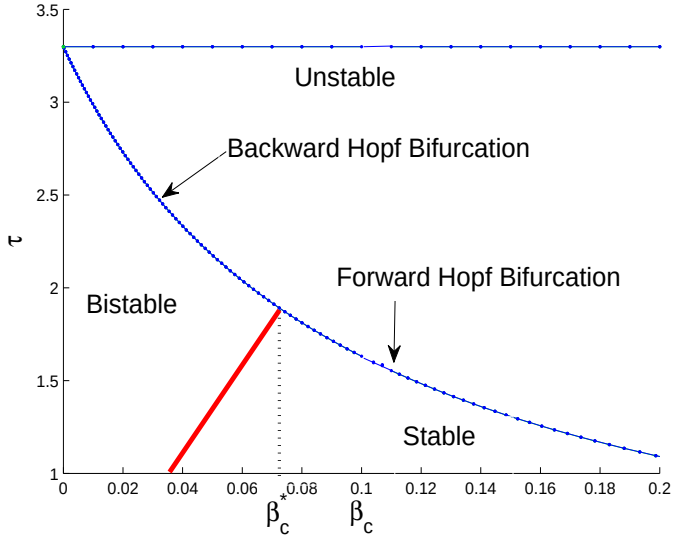

FIGURE 3.4. The branch of Hopf bifurcation in (τ, β_c)-plane. The upper line is a Hopf bifurcation branch, and the bifurcated periodic solution is unstable. Its frequency (ω_2) is the same as that for one decoupled model, and hence the corresponding bifurcation value for τ is independent of β_c. The middle line separates the (τ, β_c)-plane into stable and unstable regions of the fundamental steady state, showing that the bifurcation value for τ decreases when β_c is increasing, and also τ tends to the bifurcation value τ_0 for decoupled model as β_c approaches 0. Through this line, backward or forward Hopf bifurcation occurs, depending on the value of β_c. For any $\beta_c < \beta_c^*$, there exists an interval for τ (as indicated by the red solid line), on which the system has bistable dynamics characterized by the coexistence of a stable steady state and a stable cycle. Here $\mu = 15$, $\alpha_f^A = \alpha_f^B = 0.2$, $\alpha_a^A = \alpha_a^B = 0.7$, $\alpha_c^A = \alpha_c^B = 0.1$, $\beta_a = 0.05$, and $\beta_f = 0.2$.

Fig. 3.4 illustrates the extension the Hopf branch bifurcated from the first bifurcation point in (β_c, τ)-plane using DDE-BIFTOOL. There are several observations. First, the first Hopf bifurcation value in term of τ decreases as β_c increases, see the decreasing blue line in the middle of Fig. 3.4. This implies that enforcing the integration strength reduces the bifurcation value. Therefore, the two assets with stable prices before integration can become unstable when they are strongly coupled. Second, the sign of the first Lyapunov coefficient $c_1(0)$ changes as the intensity of integration β_c increases and exceeds the critical value $\beta_c^* \approx 0.07$, while the quantity T does not switch sign as shown in Fig. 3.5. Therefore, the direction and the stability of the bifurcation change at β_c^*. Third, there is a Bautin bifurcation (generalized

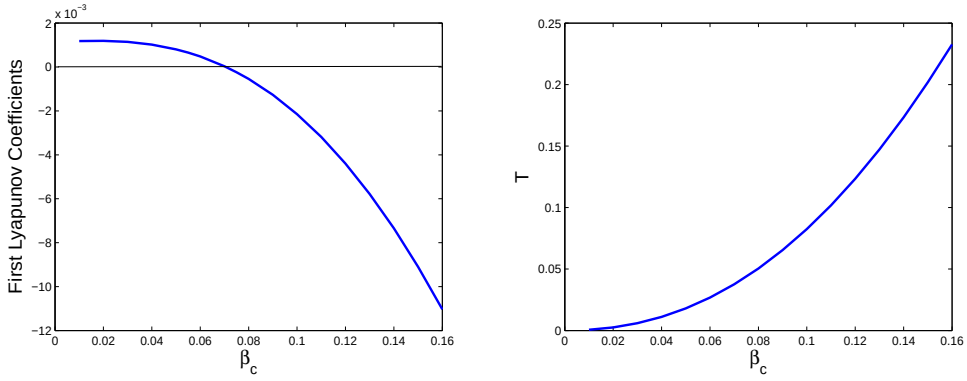

(a) $c_1(0)$ (b) T

FIGURE 3.5. (a) The first Lyapunov coefficient $c_1(0)$ and (b) the transversality condition T as functions of β_c. Here $\mu^i = 15$, $\alpha_f^A = \alpha_f^B = 0.2$, $\alpha_a^A = \alpha_a^B = 0.7$, $\alpha_c^A = \alpha_c^B = 0.1$, $\beta_a = 0.05$, and $\beta_f = 0.2$.

Hopf bifurcation) for system (3.1) at (τ_0^1, β_c^*), which theoretically implies the coexistence of two local attractors (the stable fundamental steady state and the stable limit cycle).

If both assets are unstable before coupling, then there are two series of bifurcation values introduced by the two assets respectively after market integration. For example, we consider $\tilde{\tau}_0^A < \tilde{\tau}_0^B$. Asset A becomes unstable when $\tau > \tilde{\tau}_0^A$. An interesting question following Proposition 3.3 would be whether asset B is still stable or becomes unstable for $\tilde{\tau}_0^A < \tau < \tilde{\tau}_0^B$ after integrated with asset A. The following corollary indicates the latter.

Corollary 3.5. *Assume $\gamma_c^i \neq 0$. The two prices of system* (3.1) *converge to their fundamental steady state prices or fluctuate cyclically simultaneously.*

Three observations follow Corollary 3.5. Firstly, Corollary 3.5 shows that we do not have a market situation in which one asset price converges to its fundamental price (or 'stable') and the other fluctuates cyclically (or 'unstable') simultaneously.[12] Furthermore, when the system is unstable, the bifurcated periodic solution of the two assets have the same period because the oscillation frequency is unique as demonstrated by Proposition 3.3.

[12]This is different from the observations in Chiarella, Dieci, He and Li (2013) that one asset is stable and the other can be unstable in a coupled system. Intuitively, the multi-assets are coupled via the variance-covariance matrices in Chiarella et al. (2013)'s model, which is in the higher order terms and hence cannot affect the local stability. However, the current model couples the two assets together even in its linearization skeleton. Especially, (3.1) can have such solutions that price A is stable while price B is unstable if $\gamma_c^A = 0$, which however violates the condition in Corollary 3.5.

Secondly, Corollary 3.5 also implies the spill-over effect in momentum. More specifically, consider two separate assets, one is stable and the other is unstable, that is, one has no trend and the other has (time series) momentum effect. After market integration when agents diversify their portfolios, Corollary 3.5, together with Proposition 3.4, shows that the stable asset become unstable and exhibits momentum. Therefore, the momentum can spill over from one asset to another. The spillover effect in momentum is also documented empirically in Gebhardt et al. (2005) and Jostova et al. (2013). This also implies that time series momentum can give rise to cross-sectional momentum. In fact, Moskowitz et al. (2012) show that positive auto-covariance is the main driving force for time series momentum and cross-sectional momentum effects, while the contribution of serial cross-correlations and variation in mean returns is small. Furthermore, they show that time series momentum "*is able to fully explain cross-sectional momentum across all assets as well as within each asset class*", while time series momentum is not fully captured by cross-sectional momentum. Our model provides a theoretical support to these empirical results.

Thirdly, notice that (3.1) implies that P^A_{t+dt} (P^B_{t+dt}) is a decreasing function of P^B_t (P^A_t). An increase in one asset price tends to decrease the other's price. The countercyclical behavior of the two asset prices is caused by the cross-sectional momentum trading. In other words, cross-sectional momentum trading makes the two asset's returns tend to be negatively correlated, which in turn amplifies cross-sectional momentum effect. Therefore, cross-sectional momentum trading tends to be self-fulfilling.[13]

In all, we show that the cross-sectional momentum trading, which integrates the two asset dynamics, can change both local and global dynamics by making the two price dynamics resonance.

3.3. **The Impact of Cross-sectional Trading on the Bistable Dynamics.** We further explore how integration effect affects the dynamics of (3.1) by numerically studying different dynamics of the two assets before integration.

3.3.1. *Scenario A: Backward + Backward ⇒ Backward or Forward.* We first examine the case in which the two prices for assets A and B have backward and unstable bifurcations before integration. Set $\mu^i = 15$, $\alpha^A_f = 0.2$, $\alpha^B_f = 0.25$, $\beta_f = 0.2$, $\alpha^A_a = 0.7$, $\alpha^B_a = 0.65$, and $\beta_a = 0.05$. By Propositions 3.1 and 3.2, the first bifurcation values for each asset model are 3.30 (for A) and 5.21 (for B), and their first Lyapunov coefficients are 1.1×10^{-3} and 1.2×10^{-3}, respectively, implying backward and unstable bifurcations for each asset before the integration. Let $\alpha^A_c = 0.1$, $\alpha^B_c = 0.1$ and $\beta_c = 0.03$. Then, there are two frequencies $\omega_1 \approx 0.59$ and $\omega_2 \approx 0.46$

[13]He and Li (2015) also show that the time series momentum trading is self-fulfilling.

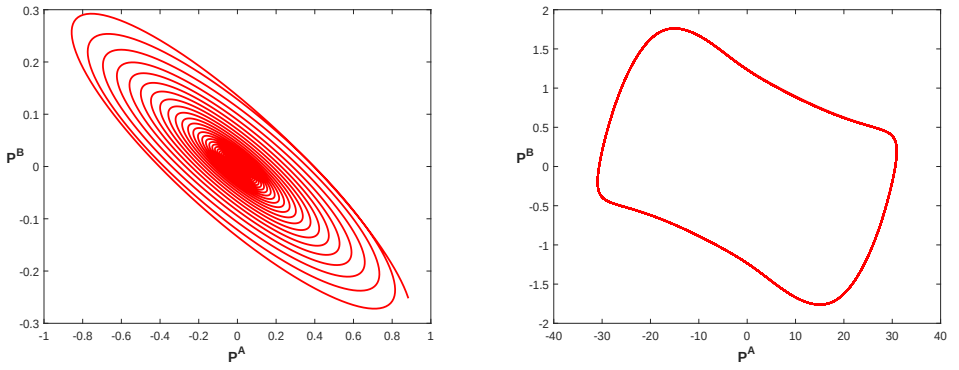

(a) Initial values $(P^A, P^B) = (2, 2)$ (b) Initial values $(P^A, P^B) = (20, 20)$

FIGURE 3.6. The solution of (3.1) for $\tau = 2.7 < 2.74$ with different initial values: (a) $(P^A, P^B) = (2, 2)$ and (b) $(P^A, P^B) = (20, 20)$ over $[-\tau, 0]$. Here $\mu^i = 15$, $\alpha_f^A = 0.2$, $\alpha_f^B = 0.25$, $\beta_f = 0.2$, $\alpha_a^A = 0.7$, $\alpha_a^B = 0.65$, $\beta_a = 0.05$, $\alpha_c^A = 0.1$, $\alpha_c^B = 0.1$, $\beta_c = 0.03$, $\bar{F}^A = 0$ and $\bar{F}^B = 0$.

for the integrated system, and their corresponding smallest bifurcation values are $\tau_0^1 \approx 2.74$ and $\tau_0^2 \approx 4.42$ respectively. Therefore, the first Hopf bifurcation value for (3.1) is $\tau_0 = \tau_0^1$, implying that the integration effect destabilizes the fundamental steady state by reducing the first bifurcation value. Furthermore, we have $T \approx 0.02$ and $c_1(0) \approx 1.0 \times 10^{-3}$ when $\tau = \tau_0$. This indicates that the Hopf bifurcation for the integrated system (3.1) at $\tau = \tau_0$ is still backward and the bifurcated periodic solution is unstable. The bistable dynamics (one locally stable fundamental steady state and one locally stable limit cycle) is illustrated in Fig. 3.6 by choosing different initial values. The opposite price dynamics for the two assets are caused by the cross-sectional momentum trading, which always longs one asset while at the same time shorts the other. In other words, the cross-sectional momentum investors tend to destabilize the cross-section of asset returns.

Changing the value of parameter β_c from 0.03 to 0.09, the first bifurcation value becomes 1.86, the transversality condition $T = 0.08$, and the first Lyapunov coefficient $c_1(0) \approx -6.0 \times 10^{-4}$, implying that the bifurcation becomes forward and the bifurcated periodic solution is stable. The bifurcation diagrams for different β_c are shown in Fig. 3.7. Note that the first Lyapunov coefficients are positive for both assets when they are decoupled, and it may become negative after integration. In this case, the integrated system only has one local attractor (periodic solution), even if there are two stable attractors (fundamental steady state and periodic solution) for each asset before integration. Therefore, the integration of the two assets tends to stabilize the otherwise unstable cycles before the integration.

Intuitively, the cross-sectional momentum trading tends to destabilize the market and strengthen the stability of the limit cycles. Therefore, as integration strength increases, the basin of the attractor of the limit cycle grows while that of the steady state declines. With strong integration, the steady state completely losses its stability and hence the backward and unstable Hopf bifurcations for the two individual assets before the integration become forward and stable after coupling.

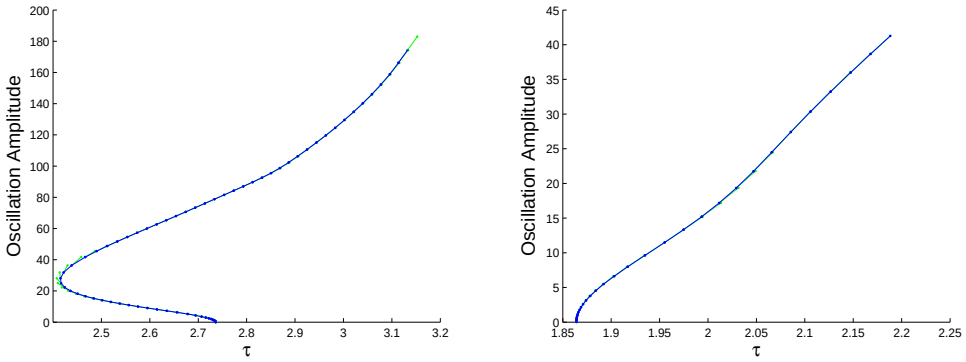

(a) $\beta_c = 0.03$ (b) $\beta_c = 0.09$

FIGURE 3.7. Hopf bifurcation extension for asset A's price of the system (3.1) in scenario A for (a) $\beta_c = 0.03$ and (b) $\beta_c = 0.09$. Here $\mu^i = 15$, $\alpha_f^A = 0.2$, $\alpha_f^B = 0.25$, $\alpha_a^A = 0.7$, $\alpha_a^B = 0.65$, $\alpha_c^A = 0.1$, $\alpha_c^B = 0.1$, $\beta_f = 0.2$, and $\beta_a = 0.05$.

3.3.2. *Scenario B: Backward + Forward ⇒ Backward or Forward.* We choose another set of parameter values, $\mu^i = 15$, $\alpha_f^A = 0.12$, $\alpha_f^B = 0.1$, $\beta_f = 0.2$, $\alpha_a^A = 0.78$, $\alpha_a^B = 0.3$, $\beta_a = 0.084$, such that each asset model undergoes different types of Hopf bifurcations when they are decoupled. In fact, the first bifurcation value and the first Lyapunov coefficient are 1.16 (3.69) and -6.4×10^{-6} (5.4×10^{-5}) respectively for asset A (B), implying the bifurcation is forward and stable (backward and unstable) for asset A (B). Let $\alpha_c^A = 0.1$, $\alpha_c^B = 0.6$ and $\beta_c = 0.01$. Then, there exists two frequencies $\omega_1 \approx 0.79$ and $\omega_2 \approx 0.53$, with their corresponding bifurcation values given by $\tau_0^1 \approx 1.07$ and $\tau_0^2 \approx 1.95$ for the integrated system. Moreover, $T \approx 0.07$ and $c_1(0) \approx 5.6 \times 10^{-5}$ when $\tau = \tau_0 = \tau_0^1$, which implies the Hopf bifurcation for (3.1) at $\tau = \tau_0$ is backward and the bifurcated periodic solution is unstable. However, the first bifurcation value decreases after the integration.

Choosing $\beta_c = 0.06$, we obtain the first bifurcation value of 0.90, the transversality condition $T = 0.08$, the first Lyapunov coefficient $c_1(0) \approx -8.0 \times 10^{-4}$, and hence the corresponding bifurcation is forward and stable. The bifurcation diagrams are omitted, since they are similar to Fig. 3.7. Therefore, we show that Backward +

Forward ⇒ Backward. However, the first bifurcation value becomes smaller after the integration.

3.3.3. *Scenario C: Forward + Forward ⇒ Forward.* Numerical simulations (not reported here) also show that when the two asset prices have forward and stable Hopf bifurcation before the integration, the integrated system always have a forward and stable Hopf bifurcation.

In all, we have shown that the integration effect destabilizes the system in two ways. First, an increase in the integration strength parameter β_c reduces the first bifurcation value, so the fundamental steady state of the integrated system is prone to be unstable compared with the decoupled systems. Second, an increase in β_c tends to lead the cycles of the integrated system stable, even though the decoupled systems have unstable cycles.

4. Price Behaviour of the Stochastic Model

In this section, through numerical simulations, we study the interaction between the global dynamics of the deterministic model and noise processes and explore the potential power of the model to generate various market behaviour and the stylized facts observed in financial markets.

4.1. **Bistable Dynamics and Stochastic Switching.** Fig. 4.1 illustrates the time series of log market prices and log fundamental prices for assets A and B with different initial conditions. With the chosen parameters, Fig. 3.5 shows that the corresponding deterministic system has bistable dynamics, that is, the coexistence of a stable fundamental steady state and a stable cycle. When we choose the initial values close to the fundamental steady state, the prices converge to the stable fundamental steady state of the corresponding deterministic system. For the stochastic system, Figs. 4.1 (a) and (b) show that the stochastic market prices (the red solid line) follow the fundamental prices (the blue dotted line) in general, but accompanied with small deviations from time to time. However, when we choose the initial values far away from the steady state, the prices converge to the stable limit cycle of the corresponding deterministic system and the stochastic market prices fluctuate widely around their fundamentals for the stochastic system as illustrated in Figs. 4.1 (c) and (d). Further numerical simulations (not reported here) show that when we choose the initial values in between the stable fundamental steady state and the stable cycle, the fluctuations of the market prices become stronger than those in Figs. 4.1 (a) and (b) but weaker than in Figs. 4.1 (c) and (d). This illustrates a significant impact of the initial value on the price dynamics when the underlying deterministic model is bistable.

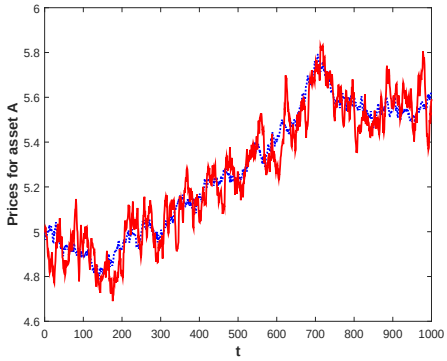

(a) Initial value of $P_s^A = P_s^B = 2$ for $-\tau \leq s \leq 0$

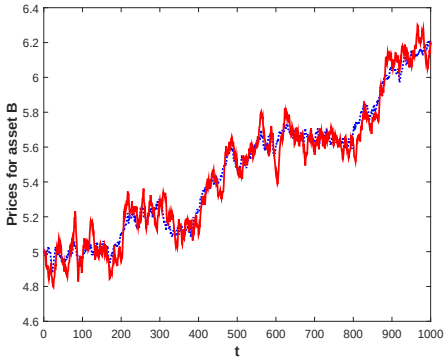

(b) Initial value of $P_s^A = P_s^B = 2$ for $-\tau \leq s \leq 0$

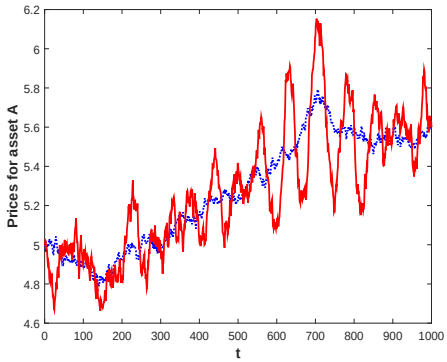

(c) Initial value of $P_s^A = P_s^B = 20$ for $-\tau \leq s \leq 0$

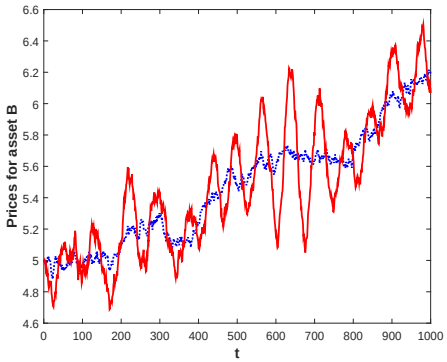

(d) Initial value of $P_s^A = P_s^B = 20$ for $-\tau \leq s \leq 0$

FIGURE 4.1. The time series of log market prices and log fundamental prices for assets A and B with different initial conditions. $\mu^A = \mu^B = 15$, $\alpha_f^A = \alpha_f^B = 0.2$, $\alpha_a^A = \alpha_a^B = 0.7$, $\alpha_c^A = \alpha_c^B = 0.1$, $\beta_f = 0.2$, $\beta_a = 0.05$, $\beta_c = 0.01$, $\sigma_{A,1}^F = 0.05$, $\sigma_{A,2}^F = 0.01$, $\sigma_{B,1}^F = 0.01$, $\sigma_{B,2}^F = 0.06$, $\sigma_{A,1}^M = 0.1$, $\sigma_{A,2}^M = 0.05$, $\sigma_{B,1}^M = 0.05$, $\sigma_{B,2}^M = 0.08$, $\bar{F}^A = \bar{F}^B = 5$ and $\tau = 2$.

4.2. **Spillover Effect.** The spillover effect in returns and volatilities has been extensively documented in the literature. It has been observed in various assets, including international equity markets (King, Sentana and Wadhwani, 1994, Forbes and Rigobon, 2002), bond markets (Christiansen, 2007), foreign exchange markets (Hong, 2001) and commodity markets (Nazlioglu, Erdem and Soytas, 2013).

We numerically examine the spillover effect by exploring the joint impact of the integration intensity β_c and the two noise processes on the market price dynamics. To examine the impact of the market integration on the stochastic price dynamics, we choose the same market volatility and fundamental volatility for the two assets.

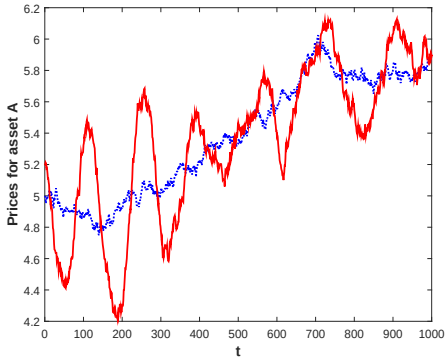

(a) Prices for A when $\beta_c = 0$

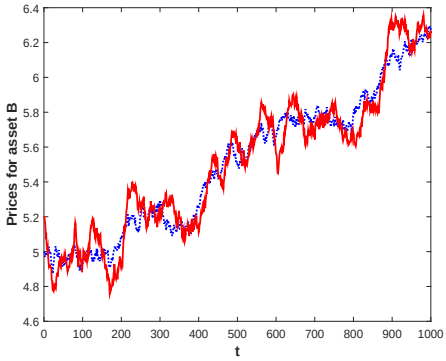

(b) Prices for B when $\beta_c = 0$

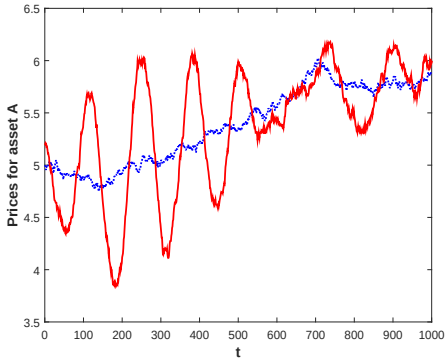

(c) Prices for A when $\beta_c = 0.015$

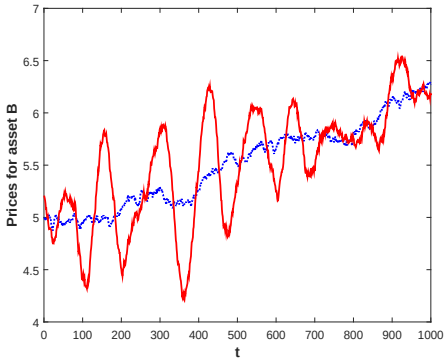

(d) Prices for B when $\beta_c = 0.015$

FIGURE 4.2. The time series of log market prices and log fundamental prices for assets A and B with different initial conditions. $\mu^A = \mu^B = 15$, $\alpha_f^A = 0.2$, $\alpha_f^B = 0.7$, $\alpha_a^A = 0.7$, $\alpha_a^B = 0.2$, $\alpha_c^A = 0.1$, $\alpha_c^B = 0.1$, $\beta_f = 0.2$, $\beta_a = 0.05$, $\sigma_{A,1}^F = 0.06$, $\sigma_{A,2}^F = 0.05$, $\sigma_{B,1}^F = 0.05$, $\sigma_{B,2}^F = 0.06$, $\sigma_{A,1}^M = 0.08$, $\sigma_{A,2}^M = 0.05$, $\sigma_{B,1}^M = 0.05$, $\sigma_{B,2}^M = 0.08$, $\bar{F}^A = \bar{F}^B = 5$, and $\tau = 2.8$.

However, we consider a situation in which the fundamental steady state of the corresponding deterministic model is unstable for asset A but stable for asset B before market integration (that is, $\beta_c = 0$). Figs. 4.2 (a) and (b) show that the stochastic price of asset A has greater fluctuations than asset B's, and the realized annual standard deviations of market returns are 9.3% and 8.6% for assets A and B respectively and the correlation is 45.3%. The higher volatility for asset A is mainly driven by the greater activity of momentum investors in asset A. Figs. 4.2 (c) and (d) illustrate the prices after market integration (that is, $\beta_c > 0$). They show that market integration increases the volatilities for both assets, and the realized annual standard deviations of market returns become 10.8% and 10.7% for assets A and B respectively. Notice the volatility for asset B increases by 24.4%, much

bigger than the increase for asset A, 16.1%. Therefore, cross-momentum trading leads to a spillover in volatility. However, the correlation between the two assets' returns reduces to 15.7%. In fact, Fig. 3.6 has shown that the cross-sectional momentum trading leads to an opposite movements of the two assets, and hence we observe smaller correlations after market integration. Therefore, the cross-sectional momentum trading reduces return correlations, which in turn make the momentum portfolios become more diversified. Further numerical simulations (not reported here) show that the correlation increases in the σ_F^{AB} and σ_M^{AB}.

We also conduct Monte Carlo simulations. Based on the set of parameters used in Fig. 4.2, and 1000 different random seeds, the average realized annual standard deviations of market returns are 8.9% and 8.5% for assets A and B respectively and the correlation is 43.5% when $\beta_c = 0$. With the cross-sectional momentum trading ($\beta_c = 0.015$), the average realized annual standard deviations of market returns become 16.4% and 16.3% for assets A and B respectively and the correlation is reduced to 28.3%. The Monte Carlo results confirm that cross-sectional momentum trading reduces return correlation.

5. Empirical Evidence from US Market

Table 5.1. Panel (A): the average correlations among stock returns before and after publication of momentum, and their difference. Panel (B): the average momentum profits before and after publication. t-statistics are reported.

	Before	After	Difference
(A) Correlation	27.1%	17.5%	-9.6%
	(111.01)	(80.87)	(-35.78)
(B) Return	20.4%	21.9%	1.5%
	(6.79)	(2.78)	

Finally we provide empirical analysis to test these model implications developed in the previous section. First, we examine if cross-sectional momentum trading tends to reduce the correlations among stocks. It is reasonable to assume that there would be an increase in the usage of cross-sectional momentum strategies after Jegadeesh and Titman published their seminal work in March 1993. In fact, Jegadeesh and Titman (2001) show that the momentum strategies continued to be profitable and that past winners outperformed past losers by about the same magnitude after the publication of their 1993 paper.[14] We examine the correlations among stock returns before and

[14]Mclean and Pontiff (2016) find a decrease of 58% in the portfolio returns of 97 variables shown by academic studies to predict cross-sectional returns after they were published academically.

after the publication of momentum. We use the stocks listed in the S&P 100 index during 03/1986-12/2015 from CRSP. We drop the stocks with less than five years data before or after 03/1993. The correlations among each two stocks are calculated for before publication (i.e. 03/1986-02/1993) and after publication (i.e. 04/1993-12/2015). There are 76 stocks considered, implying 2850 correlations in total. We find that the distribution of the correlations is very close to a normal distribution. Panel (A) of Table 5.1 reports the average correlations before and after publication, and their difference. There is an economically and statistically significant decrease (35%) in the average correlations after the publication of momentum in 03/1993. The empirical finding is consistent with our theoretical results.

Second, our model implies that the cross-sectional momentum trading is self-fulfilling in the sense that it amplifies the price trends in cross-section. We consider the momentum portfolios constructed in Daniel and Moskowitz (2016). The 10-decile momentum portfolios are formed on the basis of cumulative log returns from months $t-12$ through $t-2$ using NYSE, AMEX, and NASDAQ stocks over 01/1927-03/1013. The portfolios are value weighted and rebalanced at the end of each month.[15] We escape the momentum crashes periods of 07-08/1932, and 03-05/2009 documented in Daniel and Moskowitz (2016). Panel (B) of Table 5.1 shows that the annualized average returns to momentum strategies are 20.4% and 21.9% respectively before and after the publication of momentum, indicating an increase of 1.5% in momentum return after publication. This is consistent with the finding in Schwert (2003) that among different financial anomalies, momentum is the only persistent anomaly even after its publication. In fact, the abnormal returns even increase after its publication. Jegadeesh and Titman (2001) also show that the relative returns to high-momentum stocks increased after their publication of momentum. We also find similar results (not reported here) based on the 10-decile momentum portfolios in Ken French's data library.[16] Therefore, more momentum trading seems not able to arbitrage away the abnormal momentum returns, however in turn amplifies the momentum profits. This supports our model implication that the cross-sectional momentum trading destabilizes the market and leads to more significant price trends in cross-section.

6. Conclusion

In this paper, we develop a continuous-time nonlinear heterogeneous agent model of multiple assets to characterize the cross-sectional momentum trading. Both local and global dynamics are examined via stability, bifurcation theory, normal form

[15]See the online appendix of Daniel and Moskowitz (2016) for the details of portfolio formation.

[16]The portfolios are constructed using NYSE prior 2-12 months return decile breakpoints. See $http://mba.tuck.dartmouth.edu/pages/faculty/ken.french/data_library.html$.

method, and center manifold theory respectively. The impact of integration is examined for different cases in which the asset dynamics have various combinations before introducing cross-section momentum trading. The bistable dynamics (or the coexistence of a local stable fundamental steady state and a local stable cycle) occur through a Bautin bifurcation (generalized Hopf bifurcation). We show that, in addition to the loss of local stability of the fundamental steady states, momentum trading destabilizes the market by strengthening the stability of limit cycles.

Channeled by the underlying deterministic dynamics, the stochastic price model can generate various stylized facts observed in the financial markets, including market booms and crashes, comovements and spillover effects. Our analysis suggests that cross-sectional momentum trading tends to be self-fulfilling in the sense that it destabilizes the market and amplifies the price trends in cross-section. Our analysis also suggests that cross-sectional momentum trading leads to decreases in return correlations, which in turn make the cross-sectional momentum portfolios more diversified. Empirical evidence based on US market supports our main findings.

Appendix A. A General Model with N Assets

The two-asset model (2.5) can be extended to a general case with N risky assets,

$$\begin{aligned} dP_t^i = \mu^i \Big\{ & \alpha_f^i \tanh(\beta_f f_t^i) + \alpha_a^i \tanh(\beta_a r_{t,t-\tau}^i) \\ & + \alpha_c^i \tanh\Big[\frac{\beta_c}{N}(r_{t,t-\tau}^i - r_{t,t-\tau}^m)\Big]\Big\} dt + \sigma_M^A dW_{M,t}^A, \qquad i = 1, 2, \cdots, N, \end{aligned} \tag{A.1}$$

where $f_t^i = F_t^i - P_t^i$ is the fundamental factor, $r_{t,t-\tau}^i = P_t^i - P_{t-\tau}^i$ is the return of asset i over the period of $[t-\tau, t]$ and $r_{t,t-\tau}^m = \sum_{i=1}^N r_t^i$ is the equally weighted market return. That is, the cross-sectional momentum investors buy the past winners and short the past losers over the period of $[t-\tau, t]$ simultaneously. Notice the cross-sectional momentum portfolio is an arbitrage portfolio since the total investment at time t sum to zero (Lo and Mackinlay, 1990 and DeMiguel, Nogales and Uppal, 2014). Our analysis can be straightforwardly extended to this general case, but with a more involved results.

Appendix B. Proofs

The characteristic equation at the fundamental steady state of the system 3.1 is given by

$$\big[\lambda + \gamma_f^A - (\gamma_a^A + \gamma_c^A)(1 - e^{-\lambda\tau})\big]\big[\lambda + \gamma_f^B - (\gamma_a^B + \gamma_c^B)(1 - e^{-\lambda\tau})\big] - \gamma_c^A \gamma_c^B (1 - e^{-\lambda\tau})^2 = 0. \tag{B.1}$$

B.1. **Proof of Proposition 3.1.** It is easy to verify that (3.1) has a unique steady state $P^i = \bar{F}^i$. The characteristic equation reduces to

$$\lambda + \gamma_f^i - \gamma_a^i + \gamma_a^i e^{-\lambda\tau} = 0. \tag{B.2}$$

When $\tau = 0$, (B.2) has only one negative root $\lambda = -\gamma_f^i < 0$. Substitute $\lambda = i\omega$ ($\omega > 0$) into (B.2):

$$\cos\omega\tau = 1 - \frac{\gamma_f^i}{\gamma_a^i}, \qquad \sin\omega\tau = \frac{\omega}{\gamma_a^i}, \tag{B.3}$$

leading to

$$\omega^2 = \gamma_f^i(2\gamma_a^i - \gamma_f^i). \tag{B.4}$$

If $\gamma_f^i \geq 2\gamma_a^i$, then (B.4) has no solution.

If $\gamma_f^i < 2\gamma_a^i$, then $\omega = \sqrt{\gamma_f^i(2\gamma_a^i - \gamma_f^i)}$ and

$$\tau_n^i = \frac{1}{\omega}[\cos^{-1}(1 - \gamma_f^i/\gamma_a^i) + 2n\pi], \quad n = 0, 1, 2, \cdots. \tag{B.5}$$

It is easy to verify that $\frac{d(\mathrm{Re}\lambda)}{d\tau}\Big|_{\lambda=i\omega} = \omega^2 + (\gamma_f^i - \gamma_a^i)^2 > 0$.

Therefore, the fundamental steady state P^i is locally asymptotically stable $\tau < \tau_0^i$ and unstable for $\tau > \tau_0^i$. P^i undergoes Hopf bifurcations at $\tau = \tau_n^i$, $n = 0, 1, 2, \cdots$.

B.2. **Proof of Proposition 3.2.** For the no relative momentum case, we conduct symbolic computation of the first Lyapunov coefficient, which determines the direction and stability of bifurcated periodic solutions. In this case, the prices are decoupled and the system (3.1) is given by

$$\dot{P}_t^i = \mu^i\Big[\alpha_f^i \tanh[\beta_f(\bar{F}^i - P_t^i)] + \alpha_a^i \tanh[\beta_a(P_t^i - P_{t-\tau}^i)]\Big],\ i = A, B, \tag{B.6}$$

which involves two analogical equations with different coefficients. In the following analysis, we drop the superscript i to get a scalar equation, which can represent any equation in (B.6):

$$\dot{P}_t = \mu^i\Big[\alpha_f \tanh[\beta_f(\bar{F} - P_t)] + \alpha_a \tanh[\beta_a(P_t - P_{t-\tau})]\Big]. \tag{B.7}$$

After a change of variable, $\hat{P}_t = P_t - \bar{F}$, and drop the "$\hat{}$" for ease of notation, we get

$$\dot{P}_t = -\mu^i\alpha_f \tanh(\beta_f P_t) + \mu\alpha_a \tanh[\beta_a(P_t - P_{t-\tau})]. \tag{B.8}$$

Taylor expanding the righthand side of (B.8) at 0, and then writing its linear and nonlinear parts in functional form yield:

$$L(\phi) := (\gamma_a - \gamma_f)\phi(0) - \gamma_a\phi(-\tau),$$

$$F(\phi) := \frac{1}{3}(\gamma_f\beta_f^2 - \gamma_a\beta_a^2)\phi^3(0) + \frac{1}{3}\gamma_a\beta_a^2\phi^3(-\tau) + \gamma_a\beta_a^2\phi^2(0)\phi(-\tau) - \gamma_a\beta_a^2\phi(0)\phi^2(-\tau).$$

There are mainly two methods for the first Lyapunov coefficient calculation in the literature: one is to compute the expression of center manifold (Guckenheimer and Holmes, 1983, and Hassard, Kazarinoff and Wan, 1981), and the other is to get the normal form directly via a sequence of transformation of variables without computing center manifold (Faria and Magalhaes, 1995). We use the first method by following the algorithm developed in Guckenheimer and Holmes (1983) below, which requires to compute the following quantities in the first place:

(1) the matrix-valued function $\Phi(\theta)$, satisfying $A\Phi(\theta) = \Phi(\theta)B$, where A is the infinitesimal generator of the linearized equation of (B.8), defined by

$$A\phi = \begin{cases} \phi'(\theta), & \theta \in [-\tau, 0), \\ (\gamma_a - \gamma_f)\phi(0) - \gamma_a\phi(-\tau), & \theta = 0, \end{cases}$$

and $B = \begin{pmatrix} 0, & \omega \\ -\omega, & 0 \end{pmatrix}$;

(2) the matrix-valued function $\Psi(\xi)$, satisfying $A^*\Psi(\xi) = B\Psi(\xi)$ and $(\Psi, \Phi) = I$, where A^* is the formal adjoint operator of A, defined by

$$A^*\psi = \begin{cases} -\psi'(\xi), & \xi \in (0, \tau], \\ (\gamma_a - \gamma_f)\psi(0) - \gamma_a\psi(\tau), & \xi = 0, \end{cases}$$

and $(\cdot, \cdot)$ is the bilinear form defined by

$$(\psi, \phi) = \psi(0)\phi(0) - \int_{-\tau}^{0}\int_{\xi=0}^{\theta} \psi(\xi - \theta)d\eta(\theta)\phi(\xi)d\xi;$$

(3) and the Taylor expansion, up to second order, of the expression for center manifold: $h = h_{11}(\theta)u_1^2 + h_{12}(\theta)u_1u_2 + h_{22}(\theta)u_2^2 + O(\|\mathbf{u}\|^3) := h_2 + O(\|\mathbf{u}\|^3)$, where $\mathbf{u} = (u_1, u_2)^T$ are functions of time t, standing for the coordinates of the solution to (B.8) on the center manifold.

Based on these quantities, one can derive the following ODE for $\mathbf{u}$, up to third order, on the center manifold

$$\dot{\mathbf{u}} = B\mathbf{u} + \Psi(0)F(\Phi\mathbf{u} + h_2 + O(\|\mathbf{u}\|^3)), \tag{B.9}$$

whose general form is given by

$$\dot{u}_1 = \omega u_2 + f_{11}^1u_1^2 + f_{12}^1u_1u_2 + f_{22}^1u_2^2 + f_{111}^1u_1^3 + f_{112}^1u_1^2u_2 + f_{122}^1u_1u_2^2 + f_{222}^1u_2^3 + O(4),$$
$$\dot{u}_2 = -\omega u_1 + f_{11}^2u_1^2 + f_{12}^2u_1u_2 + f_{22}^2u_2^2 + f_{111}^2u_1^3 + f_{112}^2u_1^2u_2 + f_{122}^2u_1u_2^2 + f_{222}^2u_2^3 + O(4).$$

The coefficients in the above equation depend on Φ, Ψ, h and the nonlinear term F of the original equation. According to formula in Guckenheimer and Holmes (1983),

the first Lyapunov coefficient is given by

$$\begin{aligned} c_1(0) = &\frac{1}{8}(3f^1_{111} + f^1_{122} + f^2_{112} + 3f^2_{222}) \\ &- \frac{1}{8\omega}[f^1_{12}(f^1_{11} + f^1_{22}) - f^2_{12}(f^2_{11} + f^2_{22}) - 2f^1_{11}f^2_{11} + 2f^1_{22}f^2_{22}]. \end{aligned} \tag{B.10}$$

Remark B.1. (1) The matrix Ψ satisfying both $A^*\Psi = B\Psi$ and $(\Psi_1, \Phi) = I$ is usually obtained by two steps: solving $A^*\Psi = B\Psi$ to get an intermediate matrix Ψ_1, and then multiplying it by a proper matrix K to make sure that $(\Psi, \Phi) = I$, that is, $\Psi = K\Psi_1$. Therefore, $K = (\Psi_1, \Phi)^{-1}$.

(2) The second order term in h satisfies the following system:

$$\begin{aligned} \frac{\partial h_2}{\partial \theta} + O(\|\mathbf{u}\|^3) &= \frac{\partial h_2}{\partial u} Bu + \Phi(\theta)\Psi(0)F_2(\Phi(\theta)u) + O(\|\mathbf{u}\|^3), \\ L(h_2) + F_2(\Phi(\theta)u) + O(\|\mathbf{u}\|^3) &= \frac{\partial h_2}{\partial u}|_{\theta=0} Bu + \Phi(\theta)\Psi(0)F_2(\Phi(\theta)u) + O(\|\mathbf{u}\|^3). \end{aligned}$$

which yields a series of differential equations for $h_{ij}(\theta)$, $i, j = 1, 2$, with proper boundary conditions, and hence, the approximate expression for h will be obtained by solving these equations.

Along with a similar Maple program, as in Campbell (2009), one can get

$$\Phi(\theta) = [\cos(\omega\theta), \sin(\omega\theta)],$$

$$\Psi(\xi) = \begin{bmatrix} \dfrac{-2\omega([\omega\tau\cos\omega\tau - \sin\omega\tau]\cos\omega\xi + \omega\tau\sin\omega\tau\sin\omega\xi)}{\gamma_a\omega^2\tau^2 + \gamma_a\cos^2\omega\tau - 2\omega^2\tau\cos\omega\tau - \gamma_a + 2\omega\sin\omega\tau} \\ \dfrac{-2\omega([\omega\tau\cos\omega\tau - \sin\omega\tau]\sin\omega\xi - \omega\tau\sin\omega\tau\cos\omega\xi)}{\gamma_a\omega^2\tau^2 + \gamma_a\cos^2\omega\tau - 2\omega^2\tau\cos\omega\tau - \gamma_a + 2\omega\sin\omega\tau} \end{bmatrix} := \begin{bmatrix} \psi_1(\xi) \\ \psi_2(\xi) \end{bmatrix},$$

and

$$h_2 = 0.$$

The second order term h_2 being zero is due to the fact that the second order derivatives of $\tanh x$ at $x = 0$ is 0. Substituting these variables into (B.9), also accomplished by Maple, we get

$$\begin{aligned} f^1_{111} &= \frac{1}{3}\gamma_a\beta_a^2\psi_1(0)[-1 + 3\cos\omega\tau - 3\cos^2\omega\tau + \cos^3\omega\tau] + \frac{1}{3}\gamma_f\beta_f^2\psi_1(0), \\ f^1_{122} &= \psi_1(0)\gamma_a\beta_a^2\sin^2\omega\tau(\cos\omega\tau - 1), \\ f^2_{112} &= -\psi_2(0)\gamma_a\beta_a^2\sin\omega\tau(\cos\omega\tau - 1)^2, \\ f^2_{222} &= -\frac{1}{3}\gamma_a\beta_a^2\psi_2(0)\sin^3\omega\tau, \end{aligned}$$

and all the coefficients of the second order term in (B.9) are zero. It then follows form (B.10) that the first Lyapunov coefficient is finally given by

$$c_1(0) = \frac{1}{4}\gamma_a\beta_a^2\psi_1(0)(2\cos\omega\tau - \cos^2\omega\tau - 1) + \frac{1}{8}\gamma_f\beta_f^2\psi_1(0) + \frac{1}{4}\gamma_a\beta_a^2\psi_2(0)\sin\omega\tau(\cos\omega\tau - 1). \tag{B.11}$$

B.3. **Numerical Method of the Periodic Solution Branch.** To examine these two limit cycles numerically around the Bautin bifurcation point, the scheme is to find a proper set of parameter values under which backward Hopf bifurcation happens, and then to check how the bifurcated periodic solution varies as one of these parameters (e.g. τ) changes. The choice of parameters for backward Hopf bifurcation is based on Propositions 3.1 and 3.2, while tracking the bifurcated periodic solution can be done with the aid of a Matlab package, DDE-BIFTOOL, which allows to analyse stability of steady state solutions and periodic solutions, to continue steady state fold and Hopf bifurcations, and to switch, from the latter, to an emanating branch of periodic solutions (Engelborghs, Luzyanina and Samaey, 2001). Notice the method can even numerically simulate the unstable limit cycles.

B.4. **Proof of Proposition 3.4.** The characteristic equation at the steady state $(P^A, P^B) = (\bar{F}^A, \bar{F}^B)$ is given by

$$\left[\lambda + \gamma_f^A - \gamma_c^A(1 - e^{-\lambda\tau})\right]\left[\lambda + \gamma_f^B - \gamma_c^B(1 - e^{-\lambda\tau})\right] - \gamma_c^A\gamma_c^B(1 - e^{-\lambda\tau})^2 = 0. \quad \text{(B.12)}$$

When $\tau = 0$, (B.12) has two negative roots $\lambda_1 = -\gamma_f^A$ and $\lambda_2 = -\gamma_f^B$. If $\tau > 0$, then (B.26) reduces to

$$\sin\omega\tau = \frac{-\omega N(K_1 - \omega^2) + K_2\omega L}{K_2^2\omega^2 + (K_1 - \omega^2)^2}, \quad \cos\omega\tau = \frac{-L(K_1 - \omega^2) - K_2\omega^2 N}{K_2^2\omega^2 + (K_1 - \omega^2)^2},$$

where

$$L = \gamma_f^A\gamma_c^B + \gamma_f^B\gamma_c^A,\ N = \gamma_c^A + \gamma_c^B, K_1 = \gamma_f^A\gamma_f^B - L,\ K_2 = \gamma_f^A + \gamma_f^B - N,$$

and thus ω satisfies

$$F(\bar{\omega}) = \bar{\omega}^4 + P_3\bar{\omega}^3 + P_2\bar{\omega}^2 + P_1\bar{\omega} + P_0 = 0, \quad \text{(B.13)}$$

with $\bar{\omega} = \omega^2$ and

$$\begin{aligned} P_3 &= 2(K_2^2 - 2K_1) - N^2, \\ P_2 &= 2K_1^2 + (K_2^2 - 2K_1)^2 - L^2 - (K_2^2 - 2K_1)N^2, \\ P_1 &= 2K_1^2(K_2^2 - 2K_1) - K_1^2N^2 - (K_2^2 - 2K_1)L^2, \\ P_0 &= K_1^2(K_1^2 - L^2). \end{aligned}$$

We rewrite (B.13) as

$$F_1(\bar{\omega})F_2(\bar{\omega}) = 0, \quad \text{(B.14)}$$

where

$$\begin{aligned} F_1 &= (\bar{\omega} - \gamma_f^A\gamma_f^B + \gamma_f^A\gamma_c^B + \gamma_c^A\gamma_f^B)^2 + \bar{\omega}(\gamma_f^A - \gamma_c^A + \gamma_f^B - \gamma_c^B)^2, \\ F_2 &= \bar{\omega}^2 + \bar{\omega}(\gamma_f^{A2} - 2\gamma_f^A\gamma_c^A + \gamma_f^{B2} - 2\gamma_f^B\gamma_c^B) + \gamma_f^A\gamma_f^B(\gamma_f^A\gamma_f^B - 2\gamma_f^A\gamma_c^B - 2\gamma_f^B\gamma_c^A). \end{aligned} \quad \text{(B.15)}$$

Notice $F_1 \geq 0$ and we only need to examine the positive roots of $F_2(\bar{\omega}) = 0$. We rewrite $F_2(\bar{\omega})$ as $F_2(\bar{\omega}) = \bar{\omega}^2 + a_2\bar{\omega} + b_2$, where

$$a_2 = \gamma_f^{A2} - 2\gamma_f^A\gamma_c^A + \gamma_f^{B2} - 2\gamma_f^B\gamma_c^B = K_2^2 - 2K_1 - N^2,$$
$$b_2 = \gamma_f^A\gamma_f^B(\gamma_f^A\gamma_f^B - 2\gamma_f^A\gamma_c^B - 2\gamma_f^B\gamma_c^A) = K_1^2 - L^2.$$

It is easy to verify that there is only one frequency

$$\omega_+ = \left[\frac{-a_2 + \sqrt{a_2^2 - 4b_2}}{2}\right]^{1/2}, \tag{B.16}$$

if and only if

$$(a_2, b_2) \in \{a_2^2 = 4b_2,\ a_2 < 0\} \bigcup \{b_2 < 0\} \bigcup \{a_2 < 0,\ b_2 = 0\}, \tag{B.17}$$

there are two frequencies

$$\omega_\pm = \left[\frac{-a_2 \pm \sqrt{a_2^2 - 4b_2}}{2}\right]^{1/2}, \tag{B.18}$$

if and only if

$$(a_2, b_2) \in \{a_2^2 > 4b_2 > 0,\ a_2 < 0\}, \tag{B.19}$$

and (B.15) has no positive root if and only if

$$(a_2, b_2) \in \{a_2^2 < 4b_2\} \bigcup \{a_2 = 2\sqrt{b_2}\} \bigcup \{a_2 > 0,\ b_2 = 0\} \bigcup \{a_2^2 > 4b_2 > 0,\ a_2 \geq 0\}. \tag{B.20}$$

When $b_2 \geq 0$, we get $\gamma_f^A(\gamma_f^B - 2\gamma_c^B) \geq 2\gamma_f^B\gamma_c^A$ and $\gamma_f^B(\gamma_f^A - 2\gamma_c^A) \geq 2\gamma_f^A\gamma_c^B$. Hence,

$$a_2 = \gamma_f^A(\gamma_f^A - 2\gamma_c^A) + \gamma_f^B(\gamma_f^B - 2\gamma_c^B) \geq \frac{2\gamma_f^{A2}\gamma_c^B}{\gamma_f^B} + \frac{2\gamma_f^{B2}\gamma_c^A}{\gamma_f^A} > 0,$$

which implies that the sets $\{(a_2, b_2) : a_2 < 0,\ b_2 = 0\}$ and $\{(a_2, b_2) : a_2^2 > 4b_2 > 0,\ a_2 < 0\}$ are empty. It also follows from (B.28) that the transversality condition is determined by the sign of $F'(\omega_+^2)$, which is equal to the sign of the quantity $F_2'(\omega_+^2)$ since $F_1 > 0$. If $(a_2, b_2) \in \{a_2^2 = 4b_2,\ a_2 < 0\}$, then $F_2'(\omega_+^2) = 2\omega_+^2 + a_2 = 0$. Therefore, Hopf bifurcation will never happen for $(a_2, b_2) \in \{a_2^2 = 4b_2,\ a_2 < 0\}$, and hence the sufficient condition for the occurrence of Hopf bifurcation corresponding to one frequency is $b_2 < 0$, under which $F_2'(\omega_+^2) = 2\omega_+^2 + a_2 > 0$.

Note that $\sin\omega\tau > 0$ for all positive ω, since $K_2L - K_1N = \gamma_f^{A2}\gamma_c^B + \gamma_f^{B2}\gamma_c^A > 0$. Therefore, the bifurcation value are given by

$$\tau_n = \frac{1}{\omega_+}\left[\cos^{-1}\left(\frac{-L(K_1 - \omega^2) - K_2\omega^2 N}{K_2^2\omega^2 + (K_1 - \omega^2)^2}\right) + 2n\pi\right],\ n = 0, 1, \cdots \tag{B.21}$$

The proof of the properties of Hopf bifurcation can be found in Appendix B.6 for the proof for the full model.

B.5. **Proof of Proposition 3.5.** It is sufficient to show that it cannot happens that one asset's price converges to its fundamental while the other's fluctuates cyclically simultaneously. Without loss of generality, suppose P_t^A converges to its fundamental price and P_t^B fluctuates cyclically at the same time. Because P_t^B is a cycle in this case, there exist a positive number $x > 0$ and a sequence of time $t_k,\ k = 1, 2, \cdots$, such that $t_k \to \infty$ as $k \to \infty$, and $|P_{t_k}^B - P_{t_k-\tau}^B| \geq x$.[17] The first equation of (3.1) is equivalent to

$$\begin{aligned} P_{t+dt}^A - \bar{F}^A =& P_t^A - \bar{F}^A + \mu^A \Big[\alpha_f^A \tanh[\beta_f(\bar{F}^A - P_t^A)] + \alpha_a^A \tanh[\beta_a(P_t^A - P_{t-\tau}^A)] \\ &+ \alpha_c^A \tanh\{\beta_c[(P_t^A - P_{t-\tau}^A) - (P_t^B - P_{t-\tau}^B)]\}. \end{aligned} \tag{B.22}$$

As $t \to \infty$, $\bar{F}^A - P_t^A \to 0$ and $P_t^A - P_{t-\tau}^A \to 0$ due to the convergence of P_t^A. So (B.22) implies that, for sufficiently large k,

$$|P_{t_k+dt}^A - \bar{F}^A| \approx \mu^A \alpha_c^A \tanh\{\beta_c |P_{t_k}^B - P_{t_k-\tau}^B|\} \geq \mu^A \alpha_c^A \tanh\{\beta_c x\} > 0, \tag{B.23}$$

which contradicts the assumption of the convergence of P_t^A.

This completes the proof.

B.6. **Proof of Proposition 3.3.** When $\tau = 0$, there are two roots, $\lambda_1 = -\gamma_a^A$ and $\lambda_1 = -\gamma_a^B$, for (B.1), and hence the equilibrium is locally stable. If $\pm i\omega$, $\omega > 0$ are a pair of purely imaginary roots of (B.1), then we have

$$\begin{aligned} (K_1 - \omega^2) + (L - 2M)\cos\omega\tau + \omega N \sin\omega\tau + M\cos 2\omega\tau = 0, \\ K_2\omega - (L - 2M)\sin\omega\tau + \omega N\cos\omega\tau - M\sin 2\omega\tau = 0. \end{aligned} \tag{B.24}$$

which is equivalent to

$$\begin{aligned} (K_1 - \omega^2 - M)\sin\omega\tau + K_2\omega\cos\omega\tau + \omega N = 0, \\ (K_1 - \omega^2 + M)\cos\omega\tau - K_2\omega\sin\omega\tau + (L - 2M) = 0. \end{aligned} \tag{B.25}$$

Here,

$$\begin{aligned} L &= \gamma_f^A(\gamma_a^B + \gamma_c^B) + \gamma_f^B(\gamma_a^A + \gamma_c^A), \\ M &= \gamma_a^A\gamma_a^B + \gamma_a^A\gamma_c^B + \gamma_c^A\gamma_a^B, \\ N &= \gamma_a^A + \gamma_c^A + \gamma_a^B + \gamma_c^B, \\ K_1 &= \gamma_f^A\gamma_f^B - L + M, \\ K_2 &= \gamma_f^A + \gamma_f^B - N. \end{aligned}$$

[17] We assume that τ is not equal to the multiples of the period of the cycle. Otherwise, $P_{t_k}^B - P_{t_k-\tau}^B \equiv 0$.

Therefore,

$$\begin{aligned}\sin\omega\tau &= \frac{-\omega N(K_1-\omega^2+M)+K_2\omega(L-2M)}{K_2^2\omega^2+(K_1-\omega^2)^2-M^2},\\ \cos\omega\tau &= \frac{-(L-2M)(K_1-\omega^2-M)-K_2\omega^2N}{K_2^2\omega^2+(K_1-\omega^2)^2-M^2}.\end{aligned} \tag{B.26}$$

This implies that ω must satisfy the following equation

$$\begin{aligned}&[-N(K_1-\omega^2+M)+K_2(L-2M)]^2\omega^2+[(L-2M)(K_1-\omega^2-M)+K_2\omega^2N]^2\\ =&[K_2^2\omega^2+(K_1-\omega^2)^2-M^2]^2,\end{aligned}$$

which can be simplified to

$$F(\bar\omega) := \bar\omega^4+P_3\bar\omega^3+P_2\bar\omega^2+P_1\bar\omega+P_0=0, \tag{B.27}$$

with $\bar\omega=\omega^2$, and

$$\begin{aligned}P_3 &= 2(K_2^2-2K_1)-N^2,\\ P_2 &= 2(K_1^2-M^2)+(K_2^2-2K_1)^2-(L-2M)^2-(K_2^2-2K_1)N^2+2MN^2,\\ P_1 &= 2(K_1^2-M^2)(K_2^2-2K_1)-N^2(K_1+M)^2\\ &\quad -(L-2M)^2(K_2^2-2K_1)-2M(L-2M)^2+4K_2MN(L-2M),\\ P_0 &= (K_1-M)^2(K_1+M)^2-(K_1-M)^2(L-2M)^2,\end{aligned}$$

The fundamental theorem of algebra suggests that (B.27) has four roots. The expressions of the four roots, first proposed by Lodovico Ferrari, are extremely complicated. A detailed discussion on the conditions for different cases and the corresponding solutions would be tediously long. Therefore, instead of providing a complete conditions of all possible combinations of parameters, including those economically meaningless parameter sets, we just give some simple discussions on the properties of the roots of (B.27) to provide a better understanding of the roots, and then we numerically examine the roots for certain sets of parameters we are interested in. We refer readers to Abramowitz and Stegun (1972) for the details of the formulas of the four roots. First, Vieta's Formulas show that (B.27) has even (odd) number of positive roots if $P_0>0$ (<0). Therefore, if $P_0<0$, (B.27) has at least one positive root and hence system (3.1) will undergo Hopf bifurcations. Especially, if $P_0=0$, then the number of positive roots is determined by P_2. Second, we can rewrite (B.27) as

$$(\bar\omega^2+a_1\bar\omega+b_1)(\bar\omega^2+a_2\bar\omega+b_2)=0,$$

where a_i and b_i satisfy

$$P_0=b_1b_2,\quad P_1=a_1b_2+a_2b_1,\quad P_2=a_1a_2+b_1+b_2,\quad P_3=a_1+a_2.$$

Therefore, we can instead examine the roots of the more familiar quadratic equations and the number of positive roots of (B.27) are completely determined by a_i and

b_i, $i = 1, 2$. More specifically, first, (B.27) has four positive roots if and only if $\mathbf{C}_1 \bigcap \mathbf{C}_2$, where $\mathbf{C}_i := \{a_i < 0\} \bigcap \{a_i^2 \geq 4b_i > 0\}$, $i = 1, 2$. The condition $\mathbf{C}_1 \bigcap \mathbf{C}_2$ is equivalent to $\{P_0 > 0, P_1 < 0, P_2 > 0, P_3 < 0\} \bigcap \{a_i^2 \geq 4b_i,\ i = 1, 2\}$. Second, (B.27) has two positive roots if and only if $(\mathbf{C}_1 \bigcap \overline{\mathbf{C}_2}) \bigcup (\mathbf{C}_2 \bigcap \overline{\mathbf{C}_1})$, where the overline is a complementary set operator. Third, (B.27) has no positive root if and only if $\overline{\mathbf{C}_1} \bigcap \overline{\mathbf{C}_2}$. Similarly, we can determine the conditions that (B.27) has one or three roots. To save space, we omit them. We denote $\overline{\mathbf{C}} := \overline{\mathbf{C}_1} \bigcap \overline{\mathbf{C}_2}$ as the condition that (B.27) has no positive root, so the parameter set $\mathbf{C}$ corresponds to the condition that (B.27) has at least one positive root.

Now, we consider the properties of Hopf bifurcation of system (3.1). Assume that (B.27) has positive roots, (that is, under condition $\mathbf{C}$), denoted by $\bar{\omega}_i$, i takes the integers from 1 to 4 depending on how many roots (B.27) may have. For each $\bar{\omega}_i$, one can get a sequence of bifurcation values for time delay, τ_n^i, $n = 0, 1, \cdots$, from (B.26). Denote the smallest τ_0^i for all possible i by τ_0 and the corresponding frequency by ω_0. To verify the transversality condition, set

$$G(\lambda, \tau) = \left[\lambda + \gamma_f^A - (\gamma_a^A + \gamma_c^A)(1 - e^{-\lambda\tau})\right]\left[\lambda + \gamma_f^B - (\gamma_a^B + \gamma_c^B)(1 - e^{-\lambda\tau})\right] - \gamma_c^A \gamma_c^B (1 - e^{-\lambda\tau})^2.$$

Using (B.25), we get

$$\begin{aligned}\frac{\partial G}{\partial \lambda}|_{\lambda = i\omega_0, \tau = \tau_0} = {} & [K_2 + N\cos\omega_0\tau_0 + \tau_0(K_1 - \omega_0^2 - M\cos 2\omega_0\tau_0)] \\ & + i[2\omega_0 - N\sin\omega_0\tau_0 + \tau_0(K_2\omega_0 + M\sin 2\omega_0\tau_0)],\end{aligned}$$

and

$$\frac{\partial G}{\partial \tau}|_{\lambda = i\omega_0, \tau = \tau_0} = -\omega_0(K_2\omega_0 + M\sin 2\omega_0\tau_0) + i\omega_0(K_1 - \omega_0^2 - M\cos 2\omega_0\tau_0),$$

Therefore, $\mathrm{SignRe}\left(\frac{d\tau}{d\lambda}\right) = -\mathrm{SignRe}\left(\frac{\partial G}{\partial \lambda}/\frac{\partial G}{\partial \tau}\right)$, which equals the sign of the following quantity

$$\begin{aligned}
&\omega_0[K_2 + N\cos\omega_0\tau_0 + \tau_0(K_1 - \omega_0^2 - M\cos 2\omega_0\tau_0)](K_2\omega_0 + M\sin 2\omega_0\tau_0)\\
&\quad - \omega_0[2\omega_0 - N\sin\omega_0\tau_0 + \tau(K_2\omega_0 + M\sin 2\omega_0\tau_0)](K_1 - \omega_0^2 - M\cos 2\omega_0\tau_0)\\
&= \omega_0(K_2 + N\cos\omega_0\tau_0)(K_2\omega_0 + M\sin 2\omega_0\tau_0)\\
&\quad - \omega_0(2\omega_0 - N\sin\omega_0\tau_0)(K_1 - \omega_0^2 - M\cos 2\omega_0\tau_0)\\
&= \omega_0^2(K_2^2 - 2K_1 + 2\omega_0^2) + \omega_0 K_2 M\sin 2\omega_0\tau_0 + 2\omega_0^2 M\cos 2\omega_0\tau_0\\
&\quad + K_2\omega_0^2 N\cos\omega_0\tau_0 + \omega_0 N(K_1 - \omega_0^2 + M)\sin\omega_0\tau_0\\
&= 2\omega_0^2(K_2^2 - 2K_1 + 2\omega_0^2) + 2\omega_0^2[K_2 N - (L - 2M)]\cos\omega_0\tau_0\\
&\quad + \omega_0[N(K_1 - \omega_0^2 + M) - K_2(L - 2M) - 2\omega_0^2 N]\sin\omega_0\tau_0\\
&= \frac{\omega_0^2(4\omega_0^6 + 3P_3\omega_0^4 + 2P_2\omega_0^2 + P_1)}{K_2^2\omega_0^2 + (K_1 - \omega_0^2)^2 - M^2}\\
&= \frac{\omega_0^2 F'(\omega_0^2)}{K_2^2\omega_0^2 + (K_1 - \omega_0^2)^2 - M^2} := T.
\end{aligned} \tag{B.28}$$

The computation of $c_1(0)$ in Proposition 3.3 can be done by Maple, following the same procedure as in Appendix B.2 for the single asset model. However, the expression of $c_1(0)$ is much more complicated than the one for no relative momentum model, and hence it is omitted.

Remark B.2. Although we do not provide the distribution of the roots to (B.27), we claim that (B.27) can have positive roots for certain sets of parameters. For example, assume that $\gamma_f^A = \gamma_f^B := \gamma_f$, $\gamma_a^A = \gamma_a^B := \gamma_a$ and $\gamma_c^A = \gamma_c^B := \gamma_c$. It then follows that

$$P_0 = \gamma_f^4(\gamma_f - 2\gamma_a - 2\gamma_c)^2[(\gamma_f - 2\gamma_a)^2 - 4\gamma_c(\gamma_f - 2\gamma_a)] > 0$$

when $\gamma_f - 2\gamma_a < 0$. Set $\bar{\omega}_1 = \gamma_f(2\gamma_a - \gamma_f)$. We get $F(\bar{\omega}_1) = 0$ and $F'(\bar{\omega}_1) = -32\gamma_f^2\gamma_a\gamma_c^3 < 0$. Since $\lim_{\bar{\omega}\to+\infty} F(\bar{\omega}) = +\infty$, $F(\bar{\omega}) = 0$ has at least another positive solution, denoted by $\bar{\omega}_2$, which is greater than $\bar{\omega}_1$. Assume further that the other two roots of (B.27) are non-positive. Then, $\bar{\omega}_1$ and $\bar{\omega}_2$ will determine two sequences of bifurcation values for τ, denoted by τ_n^1 and τ_n^2 respectively, $n = 0, 1, \cdots$, according to (B.26). Recall that the decoupled system ($\gamma_c = 0$) will oscillate in one side neighborhood of τ_0^i, $i = A$ or B, if $\gamma_f - 2\gamma_a < 0$. If $\tau_0^1 < \tau_0^2$, then $\tau_0^1 (= \tau_0^i)$ is the first Hopf bifurcation value, and hence the coupled system will oscillate in the same frequency as decoupled system. While $\tau_0^1 > \tau_0^2$, the first Hopf bifurcation value becomes τ_0^2, which implies that the oscillation frequency for coupled system is $\sqrt{\bar{\omega}_2}$. In this case, we conclude that two assets prices, oscillating in the same way (same

frequency and amplitude) when decoupled, will oscillate with higher frequency after integration.

References

Abramowitz, M. and Stegun, I. (1972), *Solutions of Quartic Equations*, New York: Dover, pp. 17–18. in *Handbook of Mathematical Functions with Formulas, Graphs, and Mathematical Tables*.

Amromin, G. and Sharpe, S. (2014), 'From the horse's mouth: Economic conditions and investor expectations of risk and return', *Management Science* **60**, 845–866.

Antoniou, C., Doukas, J. and Subrahmanyam, A. (2013), 'Cognitive dissonance, sentiment, and momentum', *Journal of Financial and Quantitative Analysis* **48**, 245–275.

Bacchetta, P., Mertens, E. and van Wincoop, E. (2009), 'Predictability in financial markets: What do survey expectations tell us?', *Journal of International Money and Finance* **28**, 406–426.

Barberis, N. (2013), *Psychology and the Financial Crisis of 2007-2008*, Cambridge: MIT Press. in *Financial Innovation: Too Much or Too Little?*, Eds. Haliassos, M.

Barberis, N., Greenwood, R., Jin, L. and Shleifer, A. (2015), 'X-CAPM: An extrapolative capital asset pricing model', *Journal of Financial Economics* **115**, 1–24.

Brock, W. and Hommes, C. (1997), 'A rational route to randomness', *Econometrica* **65**, 1059–1095.

Brock, W. and Hommes, C. (1998), 'Heterogeneous beliefs and routes to chaos in a simple asset pricing model', *Journal of Economic Dynamics and Control* **22**, 1235–1274.

Campbell, S. (2009), *Calculating Centre Manifolds for Delay Differential Equations Using Maple*, Springer-Verlag, New York, pp. 221–244. in *Delay Differential Equations: Recent Advances and New Directions*, Eds. Balachandran, B. and T. Kalmár-Nagy and D.E. Gilsinn.

Chiarella, C. (1992), 'The dynamics of speculative behaviour', *Annals of Operations Research* **37**, 101–123.

Chiarella, C., Dieci, R. and Gardini, L. (2002), 'Speculative behaviour and complex asset price dynamics', *Journal of Economic Behavior and Organization* **49**, 173–197.

Chiarella, C., Dieci, R. and He, X. (2009), *Heterogeneity, Market Mechanisms and Asset Price Dynamics*, Elsevier, pp. 277–344. in *Handbook of Financial Markets: Dynamics and Evolution*, Eds. Hens, T. and K.R. Schenk-Hoppe.

Chiarella, C., Dieci, R., He, X. and Li, K. (2013), 'An evolutionary CAPM under heterogeneous beliefs', *Annals of Finance* **9**, 185–215.

Chordia, T. and Shivakumar, L. (2002), 'Momentum, business cycle, and time-varying expected returns', *Journal of Finance* **57**, 985–1019.

Christiansen, C. (2007), 'Volatility-spillover effects in european bond markets', *European Financial Management* **13**, 923–948.

Chu, L., He, X., Li, K. and Tu, J. (2015), Market sentiment and paradigm shifts in equity premium forecasting, QFRC working paper 356, UTS.

Cooper, M., Gutierrez, R. and Hameed, A. (2004), 'Market states and momentum', *Journal of Finance* **59**, 1345–1365.

Daniel, K. and Moskowitz, T. (2016), 'Momentum crashes', *Journal of Financial Economics* **122**, 221–247.

DeMiguel, V., Nogales, F. and Uppal, R. (2014), 'Stock return serial dependence and out-of-sample portfolio performance', *Review of Financial Studies* **27**, 1031–1073.

Di Guilmi, C., He, X. and Li, K. (2014), 'Herding, trend chasing, and market volatility', *Journal of Economic Dynamics and Control* **48**, 349–373.

Engelborghs, K., Luzyanina, T. and Samaey, G. (2001), DDE-BIFTOOL v. 2.00: a Matlab package for bifurcation analysis of delay differential equations, technical report TW-330, Department of Computer Science, K.U.Leuven, Leuven, Belgium.

Fama, E. (1970), 'Efficient capital markets: A review of theory and empirical work', *Journal of Finance* **25**, 383–423.

Fama, E. (2014), 'Two pillars of asset pricing', *Amercan Economic Review* **104**, 1467–1485.

Faria, T. and Magalhaes, L. (1995), 'Normal forms for retarded functional differential equations with parameters and applications to Hopf bifurcation', *Journal of Differential Equations* **122**, 181–200.

Forbes, K. and Rigobon, R. (2002), 'No contagion, only interdependence: Measuring stock market comovements', *Journal of Finance* **57**, 2223–2261.

Gaunersdorfer, A., Hommes, C. and Wagener, F. (2008), 'Bifurcation routes to volatility clustering under evolutionary learning', *Journal of Economic Behavior and Organization* **67**, 27–47.

Gebhardt, W., Hvidkjaer, S. and Swaminathan, B. (2005), 'Stock and bond market interaction: Does momentum spill over?', *Journal of Financial Economics* **75**, 651–690.

Greenwood, R. and Shleifer, A. (2014), 'Expectations of returns and expected returns', *Review of Financial Studies* **27**, 714–746.

Grinblatt, M. and Moskowitz, T. (2004), 'Predicting stock price movements from past returns: The role of consistency and tax-loss selling', *Journal of Financial Economics* **71**, 541–579.

Guckenheimer, J. and Holmes, P. (1983), *Nonlinear Oscillations, Dynamical Systems, and Bifurcations of Vector Fields*, Vol. 42 of *Applied Mathematical Sciences*, Springer.

Hassard, B., Kazarinoff, N. and Wan, Y. (1981), *Theory and Applications of Hopf Bifurcation*, Cambridge University Press, Cambridge.

He, X. (2013), *Recent Developments in Asset Pricing with Heterogeneoue Beliefs and Adaptive Behaviour of Financial Markets,*, Springer, pp. 1–32. in *Global Analysis of Dynamic Models in Economics and Finance: Essays in Honour of Laura Gardini*, Eds. G.I. Bischi, C. Chiarella and I. Sushko.

He, X. and Li, K. (2012), 'Heterogeneous beliefs and adaptive behaviour in a continuous-time asset price model', *Journal of Economic Dynamics and Control* **36**, 973–987.

He, X. and Li, K. (2015), 'Profitability of time series momentum', *Journal of Banking and Finance* **53**, 140–157.

He, X., Li, K. and Li, Y. (2017), Asset allocation with time series momentum and reversal, QFRC working paper 353, UTS.

He, X., Li, K. and Wang, C. (2016), 'Volatility clustering: A nonlinear theoretical approach', *Journal of Economic Behavior and Organization* **130**, 274–297.

He, X., Li, K., Wei, J. and Zheng, M. (2009), 'Market stability switches in a continuous-time financial market with heterogeneous beliefs', *Economic Modelling* **26**, 1432–1442.

Heston, S. and Sadka, R. (2008), 'Seasonality in the cross-section of stock returns', *Journal of Financial Economics* **87**, 418–445.

Hommes, C. (2006), *Heterogeneous Agent Models in Economics and Finance*, Vol. 2 of *Handbook of Computational Economics*, North-Holland, pp. 1109–1186. in *Agent-based Computational Economics*, Eds. Tesfatsion, L. and K.L. Judd.

Hong, Y. (2001), 'A test for volatility spillover with application to exchange rates', *Journal of Econometrics* **103**, 183–224.

Jegadeesh, N. and Titman, S. (1993), 'Returns to buying winners and selling losers: Implications for stock market efficiency', *Journal of Finance* **48**, 65–91.

Jegadeesh, N. and Titman, S. (2001), 'Profitability of momentum strategies: An evaluation of alternative explanations', *Journal of Finance* **56**, 699–720.

Jostova, G., Nikolova, S., Philipov, A. and Stahel, C. (2013), 'Momentum in corporate bond returns', *Review of Financial Studies* **26**, 1649–1693.

King, M., Sentana, E. and Wadhwani, S. (1994), 'Volatility and links between national stock markets', *Econometrica* **62**, 901–933.

Kuchler, T. and Zafar, B. (2016), Personal experiences and expectations about aggregate outcomes, working paper, New York University and Federal Reserve Bank of New York.

Kuznetsov, Y. (2004), *Elements of Applied Bifurcation Theory*, SV, New York.

LeBaron, B. (2006), *Agent-based Computational Finance*, Vol. 2 of *Handbook of Computational Economics*, North-Holland, pp. 1187–1233. in *Agent-based Computational Economics*, Eds. Tesfatsion, L. and K.L. Judd.

Lo, A. and Mackinlay, A. (1990), 'When are contrarian profits due to stock market overreaction?', *Review of Financial Studies* **3**, 175–205.

Lux, T. (2009), *Stochastic Behavioural Asset Pricing and Stylized Facts*, Elsevier, pp. 161–215. in *Handbook of Financial Markets: Dynamics and Evolution*, Eds. Hens, T. and K.R. Schenk-Hoppé.

Mclean, R. and Pontiff, J. (2016), 'Does academic research destroy stock return predictability?', *Journal of Finance* **71**(5–32).

Moskowitz, T., Ooi, Y. and Pedersen, L. (2012), 'Time series momentum', *Journal of Financial Economics* **104**, 228–250.

Nazlioglu, S., Erdem, C. and Soytas, U. (2013), 'Volatility spillover between oil and agricultural commodity markets', *Energy Economics* **36**, 658–665.

Schwert, G. (2003), *Anomalies and Market Efficiency*, North-Holland, Amsterdam. in *Handbook of the Economics of Finance*, Eds. Constantinides, G.M. and M. Harris and R.M. Stulz.

Shiller, R. (2003), 'From efficient markets theory to behavioral finance', *Journal of Economic Perspectives* **17**, 83–104.

Shiller, R. (2014), 'Speculative asset prices', *American Economic Review* **104**, 1486–1517.

Vissing-Jorgensen, A. (2004), 'Perspectives on behavioral finance: Does irrationality disappear with wealth? Evidence from expectations and actions', *NBER Macroeconomics Annual* **18**, 139–194.

Wang, K. and Xu, J. (2015), 'Market volatility and momentum', *Journal of Empirical Finance* **30**, 79–91.